
Dynamic Load Evaluation of Large Dimensioned Casing Strings at Primary Cementing

Master Thesis

Author: Volker Jedlitschka

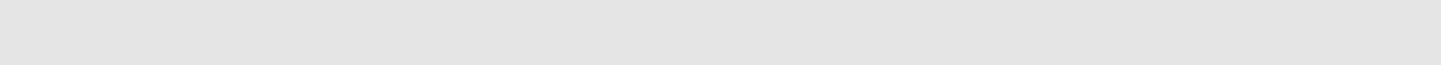
Mining University Leoben

*Chair for Drilling Engineering
in cooperation with OMV*



Industry Advisor
DI Markus Doschek

University Advisor
Univ.-Prof. DI Dr. mont. Gerhard Thonhauser



***I declare in lieu of oath that I did this
Master's thesis in hand by myself using only
literature cited at the end of this volume***

Volker Jedlitschka, Leoben in March 2007

Table of Contents

1. Acknowledgements	7
2. Zusammenfassung	8
3. Abstract	9
4. Introduction	10
5. Cementing 16” Casing at MQE-1	11
6. Free Falling Cement	15
7. Water Hammer Effect	16
7.1 What is a Water-Hammer?.....	16
7.2 Rough Estimation after Budau	16
7.3 The Elastic Liquid Column.....	18
7.3.1 Pressure Wave.....	18
7.3.2 Pressure and Fluid Velocity Distribution.....	19
7.3.3 Speed of Sound Determination.....	24
7.3.4 Dampening of the pressure waves	27
7.4 Transients in Horizontal Pipes.....	29
7.5 Transients in Vertical Pipes	31
7.6 Measuring of Pressure Waves	33
8. Water Hammer Simulation	34
8.1 Simulation with “Fluent”	34
8.2 Simulation with “Wanda 3”.....	36
9 Simulation of Water Hammer at MQE-1	41
9.1 Defining Boundary Conditions	41
9.1.1 U-Tube.....	41
9.1.2 Bonds.....	42
9.1.3 Float Collar	42
9.1.4 Free Falling Zone.....	42
9.1.5 Simulation Depth.....	43
9.1.6 Different Phases.....	43
9.1.7 Bulk Modulus.....	44
9.1.8 Cavitation Pressure.....	45
9.2 Simulation Execution	45
9.3 Simulation Results	48
9.4 Analysis – Impact of Different Parameters.....	55
9.4.1 Friction Force.....	55
9.4.2 Fluid Velocity, Fluid Density.....	57
9.4.3 Speed of Sound	57
10. Limits of Different Casing Sizes	65
11. Conclusion	67
10. References	69

List of Figures

Figure 1: Casing with landing collar lowered into the wellbore	13
Figure 2: Slurry is pumped between top and bottom plug	13
Figure 3: Top plug lands on bottom plug, cement job is done	13
Figure 4: Top and bottom plug with float collar	14
Figure 5: Situation when the water hammer possibly occurred.....	14
Figure 6: Relation between closing time and impact force according Budau	17
Figure 7: Schematic illustration according Budau4	17
Figure 8: Fluid Compression ⁶	18
Figure 9: Movement of molecules in a harmonic sound wave ⁷	19
Figure 10: Pressure and velocity sequence before the valve ⁴	21
Figure 11: Pressure and velocity sequence behind the valve ⁴	22
Figure 12: Pressure and velocity distribution along the whole pipe ⁴	23
Figure 13: Piston in a liquid filled pipe ⁷	25
Figure 14: Water hammer measured on a quick-acting valve.....	28
Figure 15: Pressure sequence caused by water hammer in horizontal pipe	30
Figure 16: Water hammer effect behind the valve	31
Figure 17: Total pressure across the valve.....	31
Figure 18: Pressure sequence at the valve, simulated in vertical pipe	32
Figure 19: Pressure sequence behind the valve, simulated in vertical pipe	32
Figure 20: Total pressure across the valve in vertical pipe	33
Figure 21: Pressure pulse set up for a pipeline	33
Figure 23: Pressure distribution along the pipe	35
Figure 24: Velocity distribution caused by the water hammer	35
Figure 25: Pressure distribution after valve has closed	36
Figure 26: "Wanda" operating windows	38
Figure 27: Pressure wave causes change in fluid velocity	38

Figure 28: Pressure wave is generated, fluid still enters pipe.....	39
Figure 29: Pressure wave propagates towards the inlet, zero fluid velocity behind the wave front.....	39
Figure 30: Wave front has reached inlet, zero fluid velocity along the pipe.....	40
Figure 31: Pressure wave was reflected, fluid exits pipe through the inlet.....	40
Figure 32: Adaption of the plug cementation to the simulation program.....	41
Figure 33: Free falling evaluation with "OptiCem".....	43
Figure 34: Fluid compression due to external pressure ¹¹	44
Figure 35: Fluid properties windows, casing fluid on the left, annular fluid on the right.....	47
Figure 36: Input Panel for pipe and valve properties.....	48
Figure 37: Water hammer effect calculated by "Wanda".....	49
Figure 38: Pressure data transferred into Excel.....	49
Figure 39: Water hammer effect behind the valve causes a negative pressure wave first.....	50
Figure 40: Load at the casing.....	51
Figure 41: Overlapping of the transient data.....	51
Figure 42: Decreasing Δp acting on the casing.....	52
Figure 43: Zoom in of figure 40.....	52
Figure 44: Discharge rate at the casing bond.....	53
Figure 45: Discharge rate at annular bond.....	54
Figure 46: Linear pressure increase due to friction force.....	55
Figure 47: Different bulk moduli affect the slope at the pressure peaks.....	56
Figure 48: Linear pressure increase on top of pressure peak.....	56
Figure 49: Water hammer simulated with higher fluid velocity.....	57
Figure 50: Pipe dimension test 1/9 (L=400m, ID=200mm).....	60
Figure 51: Pipe dimension test 2/9 (L=400m, ID=400mm).....	60
Figure 52: Pipe dimension test 3/9 (L=400m, ID=600m).....	60
Figure 53: Pipe dimension test 4/9 (L=600m, ID=200mm).....	61
Figure 54: Pipe dimension test 5/9 (L=600, ID=400mm).....	61
Figure 55: Pipe dimension test 6/9 (L=600m, ID=600mm).....	61
Figure 56: Pipe dimension test 7/9 (L=800m, ID=200mm).....	62

Figure 57: Pipe dimension test 8/9 (L=800m, ID=600mm).....	62
Figure 58: Pipe dimension test 9/9 (L=800m, ID=600mm).....	62
Figure 59: Pipe dimension test regarding wall thickness	63
Figure 60: Water hammer effect if the well would have been 10.000m deep	64
Figure 61: Tendency of the critical flow rate for several casings at certain depths	66
Figure 62: Δp caused by water hammer acting on the casing	67

1. Acknowledgements

The author would like to thank Univ.-Prof. DI Dr.mont. Gerhard THONHAUSER and DI Hermann F. SPÖRKER for their permission to write this thesis. Special thanks to DI Markus DOSCHEK from OMV and DI Dr.techn. Dominik MAYR from the Technical University Graz, Austria, for their excellent support and valuable comments during preparation of this thesis.

Strong appreciation also goes to the institute for hydraulic engineering and water resources management at the Technical University Graz, which enabled and supported the simulation with "Wanda".

Also thanks to Stefan FUHRMANN, Halliburton Company Austria, who enabled the use of OPTICEM Simulator and thus provided valuable information for this investigation.

2. Zusammenfassung

In dieser Diplomarbeit wurde eine Plug-Zementation eines 16" Casing Stranges untersucht bei der die 2440m lange Verrohrung leck wurde. Die Ursache dafür ist ungeklärt, jedoch vermutet man, dass ein sogenannter Wasserschlag den Casing beschädigte. Es wird angenommen, dass der Bottom-Plug das Rückschlagventil in der Landeplatte blockiert hat wodurch die Zementsäule zum abrupten Stillstand gekommen ist. In dieser Arbeit wird untersucht ob die Belastung, die durch einen eventuellen Wasserschlag hervorgerufen wurde, ausreichen würde um eine 16" Verrohrung zu beschädigen.

Es konnte festgestellt werden, dass eine maximale Belastung der Verrohrung von 61,53 bar aufgetreten ist, von denen jedoch nur 11,2 bar auf das Phänomen des Wasserschlages zurückzuführen sind. Diese maximale Belastung ist nicht ausreichend um den 16" Casing zu beschädigen.

Weiters würde nachgewiesen, dass im Falle eines Wasserschlages ein größerer Rohrdurchmesser nicht zu einer höheren Belastung führt sondern das Verhältnis Innendurchmesser (D) zu Wandstärke (t) entscheidend ist. Generell führt ein größeres D/t Verhältnis zu einer Reduktion des Wasserschlages.

Für üblich verwendete Casing Größen würde im Zuge dieser Arbeit festgestellt, dass größere weniger gefährdet sind, auf Grund der Belastung eines Wasserschlages zu gebrechen. Diese Tendenz konnte für verschiedene Längen festgestellt werden.

Die Ergebnisse dieser Arbeit würden mit Hilfe des Simulationsprogrammes "Wanda 3" ermittelt.

3. Abstract

In this thesis a plug cementation of a 16" casing string is investigated. What happened was that during primary cementing of a 16" casing string at a depth of 2440m the string failed. It was assumed that the bottom plug plugged the float valve and thus the cement column was immediately stopped on its way downhole. The phenomenon when fluid flow is immediately stopped is called "water hammer-effect". Task was to investigate if this water hammer effect caused a sufficient high load to damage the casing string.

It could be figured out that the string faced a maximum load of 61,53bar but out of this only 11,3bar were generated by the water hammer. The remaining 50,3bar were caused due to the hydrostatic difference between the annulus filled with mud and the casing filled with cement. It is obvious that the calculated load was not sufficient to harm the casing string.

Further it could be proved that a larger casing diameter does not compulsorily increase the impact of a water hammer. Concerning pipe dimensions the ratio between wall thickness and inner diameter is decisive. General can be said that a higher D/t ratio reduces the water hammer impact.

Concerning commonly used casing dimensions it could be proved for different lengths that larger casings are less endangered to fail due to the load caused by a water hammer.

The whole study is supported with a simulation software called Wanda 3.

4. Introduction

Decisive for the topic of this thesis was a certain failure at an OMV well drilled in 2005. What happened was that during primary cementing of a 16" casing string at a depth of 2440m, the string failed. The reason for this failure is not clear but a certain theory is investigated in this thesis. It is assumed that the bottom plug plugged the float valve at the landing collar which caused the moving cement column to be stopped immediately.

The phenomenon when fluid flow within a pipe is suddenly stopped is called "water hammer" and can lead to significant pipe damage.

The author investigates the water hammer theory in case of the 16" casing string. This study is supported by several simulation programs as "OptiCem", "Fluent" and "Wanda".

All parameters that influence this water hammer phenomenon are discussed and different casing dimensions are investigated to this effect.

After a detailed explanation of the occurrences during cementing operations, the free falling cement phenomenon is shortly explained and followed by chapters with detailed investigations.

Task is to find out if the impact of a possible water hammer would be sufficient high to damage the 16" casing string.

5. Cementing 16" Casing at MQE-1

The 18-1/2" hole section was drilled to the desired depth of 2444m and the 2440m casing string could be landed with a mandrel hanger into the wellhead with full string weight of 300tons, which was indication for a well shaped bore hole without significant drag.

For the cementing operation two 2" lines from the cement pump to the cementing head where installed. The operation was a plug cementation. In Figures 1-3 this type of cementation is schematically illustrated and in figure 4 a pair of plugs is shown. The red plug (bottom plug) is loaded, afterwards the black one (top plug).

The cementation started by pumping 16m³ of spacer (1,05kg/l) before the bottom plug was loaded. 136m³ of lead cement (1,5kg/l) and 12,7m³ tail slurry (1,9kg/l) followed. As the bottom plug landed on the float collar in time, a sudden increase in pump pressure to 120bar was observed. An abrupt pressure drop followed and circulation could be regained. At this point it was assumed that the pressure peak was caused by the membrane in the bottom plug, which normally bursts at a small pressure difference (3-7bar). It was supposed that the cement was now displaced into the annulus as usual, passing by float collar and casing shoe.

At a successful plug cementation the top plug moves downhole and when it reaches the bottom plug a pressure increase is observed at surface because the mud is pumped into a closed system. The top plug upon the bottom plug closes the system and usually at this point of time the job is done.

At OMV's well this expected pressure increase was detected a bit earlier as expected. At next the pumps were stopped and it was attempted to re-bump the plug. By doing so, continuous circulation could be established with return rates and pressure values similar as before. A continuous pressure increase could be recorded while the displacement process was continued. It has to be mentioned that the displacement was performed with the rig pumps and the pump efficiency was picked wrong as post-analysis had proven. As the risk of overdisplacement was given a close look to the mud returns from annulus were taken and unplanned spacer returns have been detected. It was planned that spacer and cement will not reach surface. The displacement process was stopped by shut-off the pumps and the pressure was released. Then the return valve on the pump was opened to check if mud was returning from the casing. If the system is tight this should not be the case and the pressure at surface should be zero. At this point normally the hydrostatic is the only pressure acting inside the casing after the top plug was landed and the pump pressure is released.

However, mud returned when the return valve at the pump was opened. This was an indication that some flow from the annulus entered the casing somewhere downhole. It has to be mentioned that a double valve float shoe and a single valve float collar were installed.

Theoretically two possible scenarios could have been happening. Either all three float valves failed or the casing itself became leak.

At this point it was decided by on-site personnel to attempt displacing the full cement volume back to surface to potentially be able to pull the 16" casing again. While further circulating communication was established with the operations office and it was decided not to displace the cement out of the annulus but let as much slurry as possible flow back (natural flow direction was from the annulus into the casing). Indeed the over displaced fluid was able to flow back into the casing string, with remarkable returns at surface from inner casing. This was an indication for a large leakage or an even parted casing string. But after several barrel of return the flow stopped and cement hardening phase started.

The next step was to examine the tightness of the casing string by running a packer. Step by step the packer was lowered and pressure tests were executed. Actually below deepest packer setting depth close to the landing collar a leakage could be detected. However, the packer became stuck close to the landing collar and could not be retrieved any more. More and more it seemed that the string had in fact been parted. It was decided to go on with a sidetrack because further examination could not change the situation on site.

After these occurrences the casing manufacturer was inspected by a third party. However no lack in quality at the manufacturing process was discovered.

Analyzing of what happened and searching for explanations the water hammer-theory came up which is graphically illustrated in Figure 5. This theory is based on the assumption that the bottom plug somehow plugged the float valve of the landing collar. This can happen either that the membrane of the plug did not burst or the plug faced so much wear on its way downhole that it parted and some rubber elements plugged the valve. Theoretically a water hammer could lead to casing burst or slippage of an improper made up casing connection.

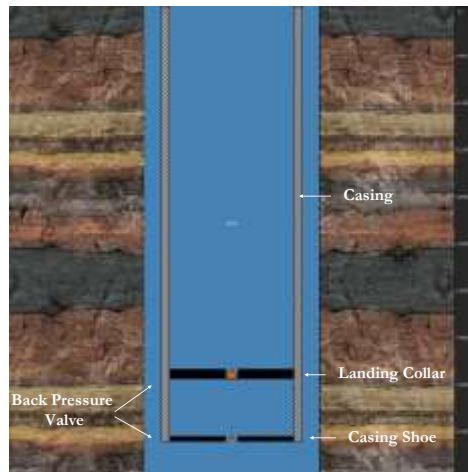


Figure 1: Casing with landing collar lowered into the wellbore

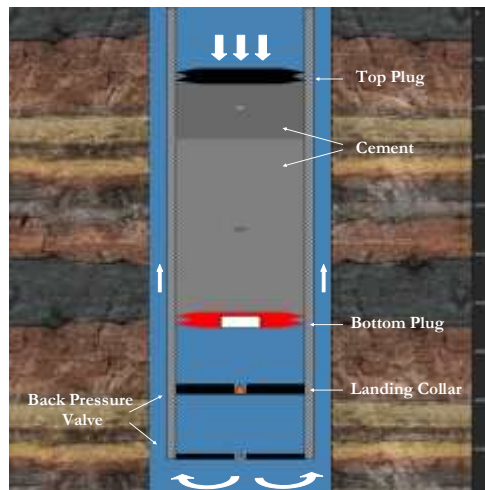


Figure 2: Slurry is pumped between top and bottom plug

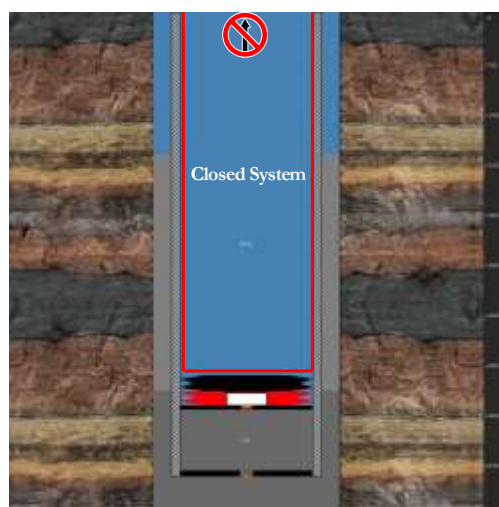


Figure 3: Top plug lands on bottom plug, cement job is done



Figure 4: Top and bottom plug with float collar

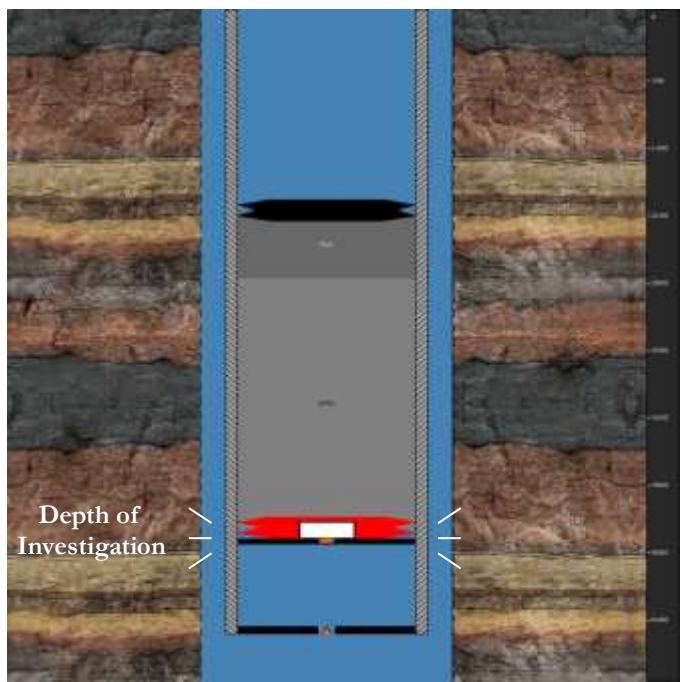


Figure 5: Situation when the water hammer possibly occurred

6. Free Falling Cement

Before discussing the water hammer effect the free falling cement phenomenon should be contemplated and well understood, which also occurred during the plug cementation of the 16" casing. It is introduced in this chapter.

Generally can be said that while cementing we have to deal with several fluids of different densities, the initial mud, a pre-flush, a spacer, various densities of cement slurries and at the end some mud again. Normally the cement slurry has a higher density as all other fluids pumped into the hole.

During the cementing process, after the plugs are loaded and pumping the cement is started, a heavier fluid column is placed above a lighter one. Besides the pump pressure, this density difference causes an additional driving force due to gravity. As pumping continues the cement column gets heavier and might start to speed up on its way downhole. Due to its acceleration it loses contact with the surface pump rate. This happens, if the total friction pressure is exceeded by the hydrostatic pressure difference between the fluid column inside the casing and the fluid column in the annulus¹. These conditions in the wellbore lead to a phenomenon called "free falling cement". This free falling period of the cement has several consequences and is highly influenced by differences in fluid densities and depth. It causes a negative absolute well head pressure, which lead to a discontinuous zone between the well head and the free falling column¹. This means the fluids do not occupy the entire pipe diameter any more.

The free falling cement phenomenon was quite detailed investigated by Beirute² in 1987 and by Spörker¹ in 1993. In several field studies and simulation runs Spörker analyzed the cementing head pressures, pump rates and return rates versus time and could exactly define when free falling actually occurs and how long this period lasts. Spörker monitored that when the well head pressure drops during the cement job the annular return rates exceed the pump rates. That means more fluid returns from the annulus as it is pumped into the well. Now the free falling period has started. Further more it was observed by Spörker that towards the end of the job the situation reverses and it seems that a lost circulation condition occurs. At this time, when the cement enters the annulus through the casing shoe, the fluids create their own equilibrium between friction and hydrostatic forces¹. This is called U-tubing. As pumping continues, this equilibrium will never be a static one but pump rates have no longer influence on the fluid velocity.

Concerning the displacement process in the annulus, during the cementation job, the free falling period itself does not matter that much. What matters is that the slow movement of the slurry in the annulus during the later stages avoids satisfying displacement, as displacement efficiency is a function of the displacing fluid velocity¹.

For this study it is important to understand the free falling phenomenon, not because of the displacement efficiency, but with regard to the fluid velocities within the pipe.

7. Water Hammer Effect

Since it is assumed that a kind of water-hammer effect could be the reason for the failure of the 16" casing, it is detailed investigated in this chapter.

7.1 What is a Water-Hammer?

Water hammer or hydraulic shock is a momentary increase in pressure and is the result of a sudden change in liquid velocity. A water hammer usually occurs when a transfer system is quickly started, stopped or is forced to make a rapid change in direction. Following points are common reasons for a water hammer effect:

- Valve operations
- Pumps switching on or off
- Filling up of pipes
- Irregular pumping (discontinuous suction of air)

The primary cause of water hammer in process applications is the quick closing and opening of a valve. A valve is defined as quick acting if it closes before a pressure wave is reflected back from upstream or down stream. Symptoms include noise, vibration and hammering pipe sounds which can lead to equipment damage. A common example of a water hammer in most homes is simply turning off a shower quickly. By doing so, a thud through the house piping can eventually be recognized. The magnitude of the water hammer is mainly influenced by the change of flow. The quicker a valve is operated the higher the impact.

The generated shock wave (transient) is caused by the kinetic energy of the fluid in motion when it is forced to stop suddenly. Moving water in a pipe has kinetic energy proportional to the mass of water in a given volume times the square of its velocity³.

$$\text{kinetic energy} = (\text{mass} \times \text{velocity}^2)/2 \quad (1)$$

If the velocity becomes zero cause of such reasons mentioned above, there is still energy left. This energy changes in deformation energy and is transferred to the piping and the medium itself (liquid in this case). For this reason, most pipe sizing charts recommend to keep the flow velocity below 1,5m/s³.

7.2 Rough Estimation after Budau

This estimation considers a liquid column as a rigid body with the mass m ⁴. The mechanics of rigid bodies tells us that a change in velocity of a mass causes a force F :

$$m \cdot \frac{dv}{dt} = F \quad (2)$$

If the velocity with the initial value of v_0 changes to a final value of v_e while the valve is closing, the integration of Equation (2) delivers:

$$m \cdot v_0 - m \cdot v_e = \int_0^T F \cdot dt \quad (3^4)$$

In this relation the valve closing time is expressed with T . In order to solve Equation (3) the function $F(t)$ has to be known. Strictly spoken this function can only be evaluated from the operating characteristic of a valve, which describes the change in cross-sectional area

while closing. For a rough approximation Budau suggests to use a quadratic relation between the force F and the time t (Figure 6).⁴

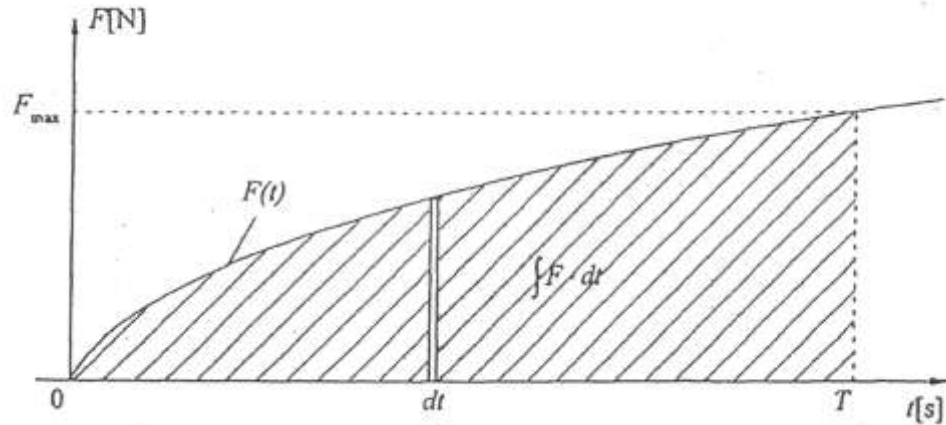


Figure 6: Relation between closing time and impact force according Budau

In a F, t - coordinate system the integral $\int_0^T F \cdot dt$ illustrates the area below the curve and due to its parabolic shape it can be determined by following relation:

$$\int_0^T F \cdot dt = \frac{2}{3} \cdot F_{\max} \cdot T = m \cdot v_0 - m \cdot v_e \quad (4^4)$$

For a pipe with a length l and a cross sectional area A the mass of the liquid can be defined as

$$m = \rho \cdot A \cdot l \quad (5)$$

and from Equation (4)

$$F_{\max} = \frac{3}{2} \cdot \frac{\rho \cdot A \cdot l \cdot (v_0 - v_e)}{T} \quad (6)$$

can be evaluated.

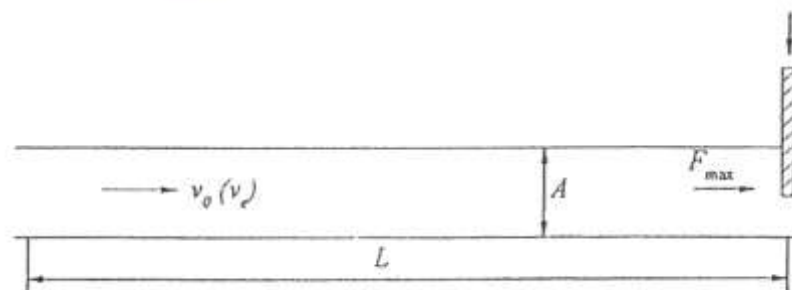


Figure 7: Schematic illustration according Budau⁴

Since $\frac{F_{\max}}{A} = P_{\max}$, the maximum pressure according Budau is defined by:

$$P_{\max} = \frac{3}{2} \cdot \frac{\rho \cdot l \cdot (Q_0 - Q_e)}{A \cdot T} \quad (7^A)$$

From Equation (7) can be seen that the pressure is higher the smaller Q_e is and the shorter the closing time is. A longer pipe also leads to a pressure increase. However, for $T \rightarrow 0$ it would mean that the pressure would become infinite high, which is not valid in praxis.

7.3 The Elastic Liquid Column

Considering the elasticity of a fluid column leads to a complete different calculation model, which includes the wave character of a pressure change ⁴.

By analyzing what exactly happens during such a water hammer, it can be said that a column of liquid, either horizontal or vertical, acts like a train crashing into a rock side ⁵. The back of the train continues forward even though the front can not go any further. In Figure 8 fluid compression is illustrated.

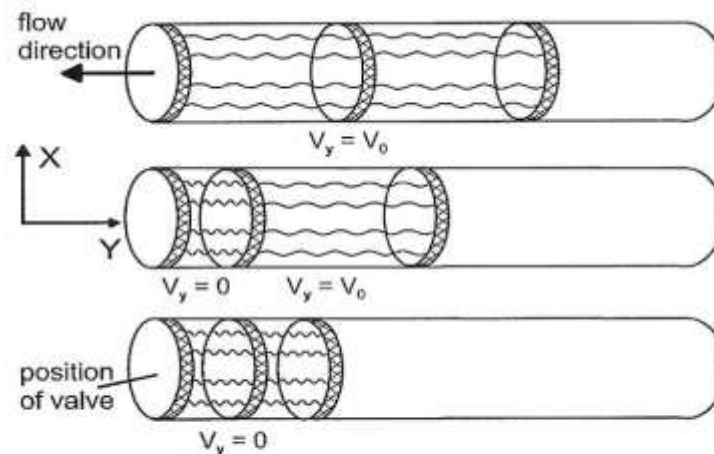


Figure 8: Fluid Compression ⁶

Since the water flow is restricted inside the pipe, a shock wave travels backward the pipe, deflecting everything in its path, then forward and back again. It is reflected at the open end of the pipe, at a wall or at a closed end pipe. By acting against the piping and valves very high forces are exerted. The pressure wave immediately accelerates to the speed of sound ⁶.

7.3.1 Pressure Wave

A pressure wave is nothing else as a sound wave. A sound wave is a wave type propagation of pressure and density changes in an elastic medium as gas, liquids or solids. Pressure waves spread as longitudinal waves. A density disturbance propagates by the

interaction between the molecules which oscillate parallel to the direction of expansion. Oscillation means that the molecules stay at their place but move around their neutral position⁷.

Figure 9 shows the movement of air molecules in a harmonic sound wave.

- Oscillation of the molecules from their state of equilibrium at a certain time point as a function of distance. The molecules at the points x_1 and x_3 stay in their state of equilibrium and those at x_2 face maximum deflection.
- Some representative molecules in their state of equilibrium before the sound wave is going to deflect them. The arrows show the direction of oscillation.
- Position of the molecules after the sound wave met them.
- Density of air at this specific time point. At the point x_3 air's density is at a maximum and at point x_1 at a minimum. At both point the oscillation of the molecules is zero.
- Change in pressure as a function of distance. It can be seen that the pressure curve (e) and the oscillation curve (a) have a phase difference of 90° .

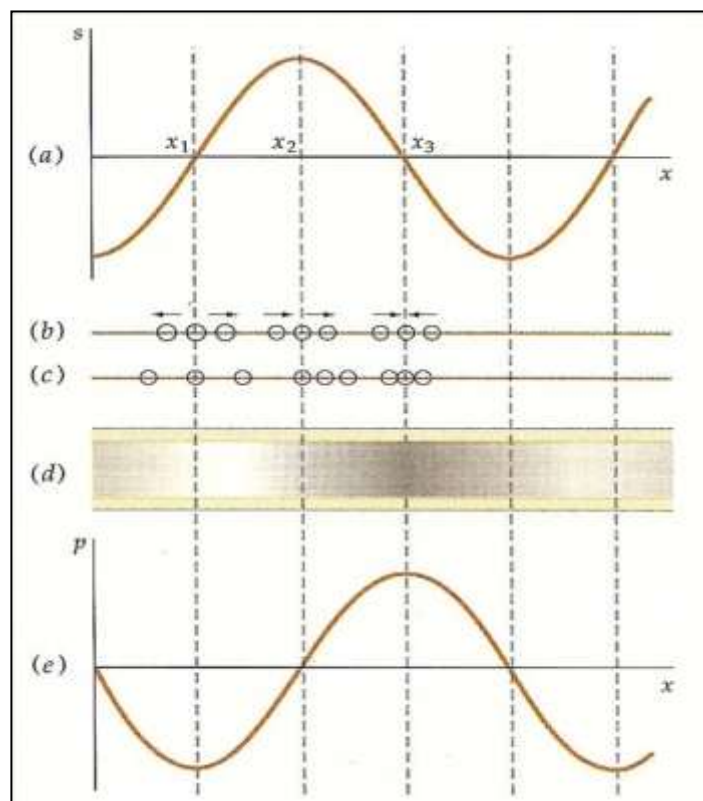


Figure 9: Movement of molecules in a harmonic sound wave⁷

In pipes not only the elasticity of water but also the one of the pipe material influences the pressure wave velocity. A pressure increase of the liquid column causes an enlargement of the pipe diameter. Due to the internal pressure, the pipe tends to expand. This effect causes a slower wave spreading in pipes as in open water systems⁷.

7.3.2 Pressure and Fluid Velocity Distribution

The following description is illustrated in Figure 10⁴. We consider a pipe which is at one end connected to a bond with water and on the other end a valve is installed. In steady state conditions water is flowing at velocity w_0 . At the time point $t=0$ the valve is closed

abruptly. This causes the velocity directly in front of the valve to become 0. The inertia of the following water particles cause a pressure increase which leads to an enlargement of the pipe diameter at the same time. This procedure now shifts with the speed of sound from the closed valve towards the pipe inlet. The pressure wave reaches the bond at the time

$$t = \frac{L}{a} .$$

In the bond the pressure wave is reflected at the liquid surface which is phase boundary to air. In hydraulic engineering a liquid surface is considered as a body of infinite inertia. This means for a pressure wave a liquid surface acts like a solid medium.

At this point of time when the wave is reflected an unbalanced situation at the transition zone between the cross sectional area of the pipe and the bond occurs. In the pipe the velocity is zero, but the pressure is higher as it is in the bond before the transition zone, where it is determined by the liquid level inside. The consequence of this situation is that the fluid starts to flow from the pipe into the bond. From the higher pressurized area to the area with lower pressure. Thereby the pressure energy again converts completely into kinetic energy again. This procedure again transfers into the pipe and reaches the valve at

$$t = \frac{2 \cdot L}{a} .$$

At this point of time an unbalanced situation occurs at the valve. The fluid flow out of the pipe into the bond now causes a suction force at the valve because no more fluid can enter through the closed valve. The suction force reduces the pressure which becomes smaller as it was at steady state flowing conditions at time point $t = 0$. Due to the suction force the pipe is compressed and therefore its diameter is reduced. Again this procedure shifts at speed of sound along the pipe and reaches the bond at

$$t = \frac{3 \cdot L}{a} .$$

The unbalanced situation now is characterised as the pressure in the bond is higher as it is in the pipe. The conversion of the pressure energy creates again a fluid velocity w_0 when the fluid enters the pipe. The fluid front and the reflected pressure wave move towards the valve. At the time

$$t = \frac{4 \cdot L}{a}$$

when the fluid reaches the valve with its velocity w_0 the same physical state is obtained as at $t = 0$. The described oscillation starts again from the beginning and lasts until the energy is consumed by friction losses. In the following Figures 10 to 12 the described pressure and velocity changes are illustrated.

Considering what is going on behind the valve a kind of reverse but similar procedure is valid. The immediate interruption of fluid flow causes a negative pressure wave behind the valve and the pipe tends to shrink. A negative pressure wave means that the pressure is smaller than at steady state conditions whereas it is termed "positive" when the pressure is higher. The fluid velocity between the shifting wave and the valve is zero and between wave and the end of the pipe is still the initial w_0 . When the negative pressure wave reaches the end of the pipe at

$$t = \frac{L}{a}$$

the fluid velocity along the whole pipe is 0. The following process is the same as for the pipe section before the valve.

It can be noticed that when the water hammer occurs the valve has to withstand a positive pressure upstream and a negative one downstream at the same time.

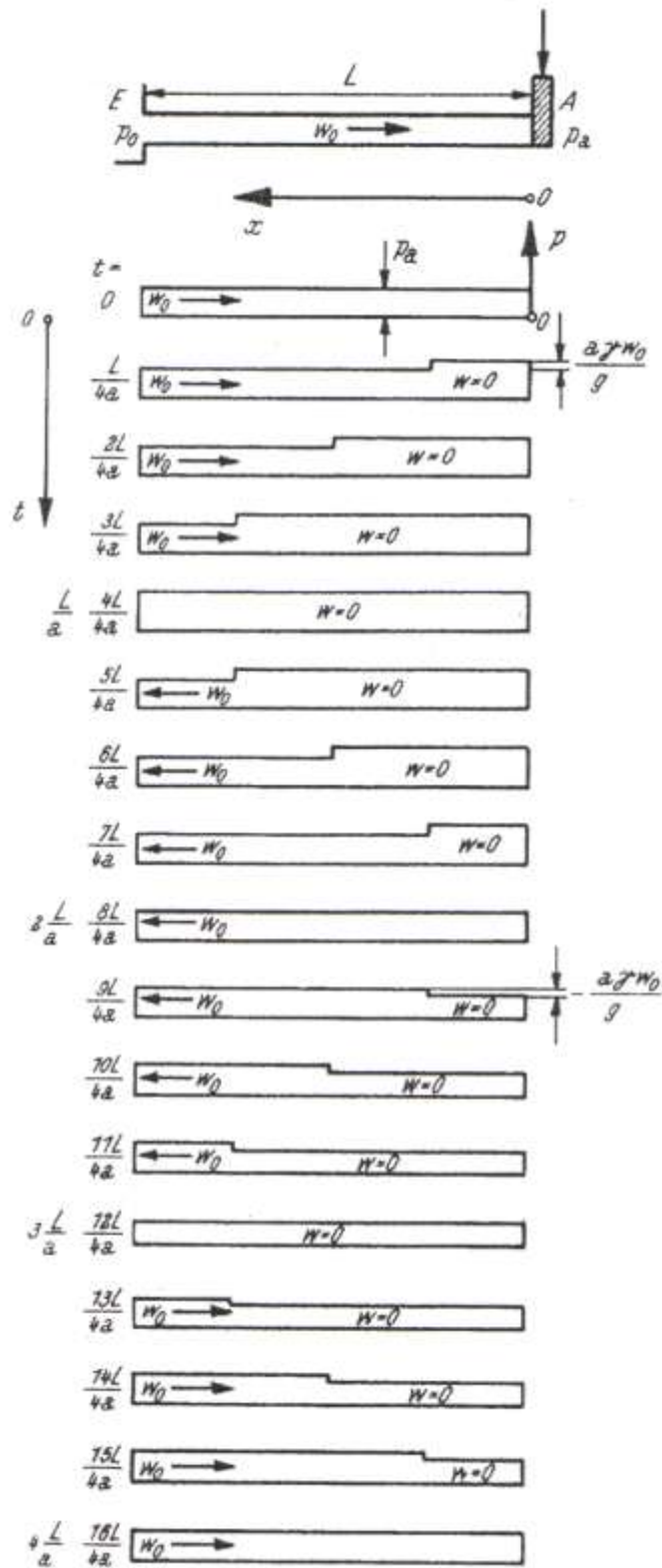


Figure 10: Pressure and velocity sequence before the valve⁴

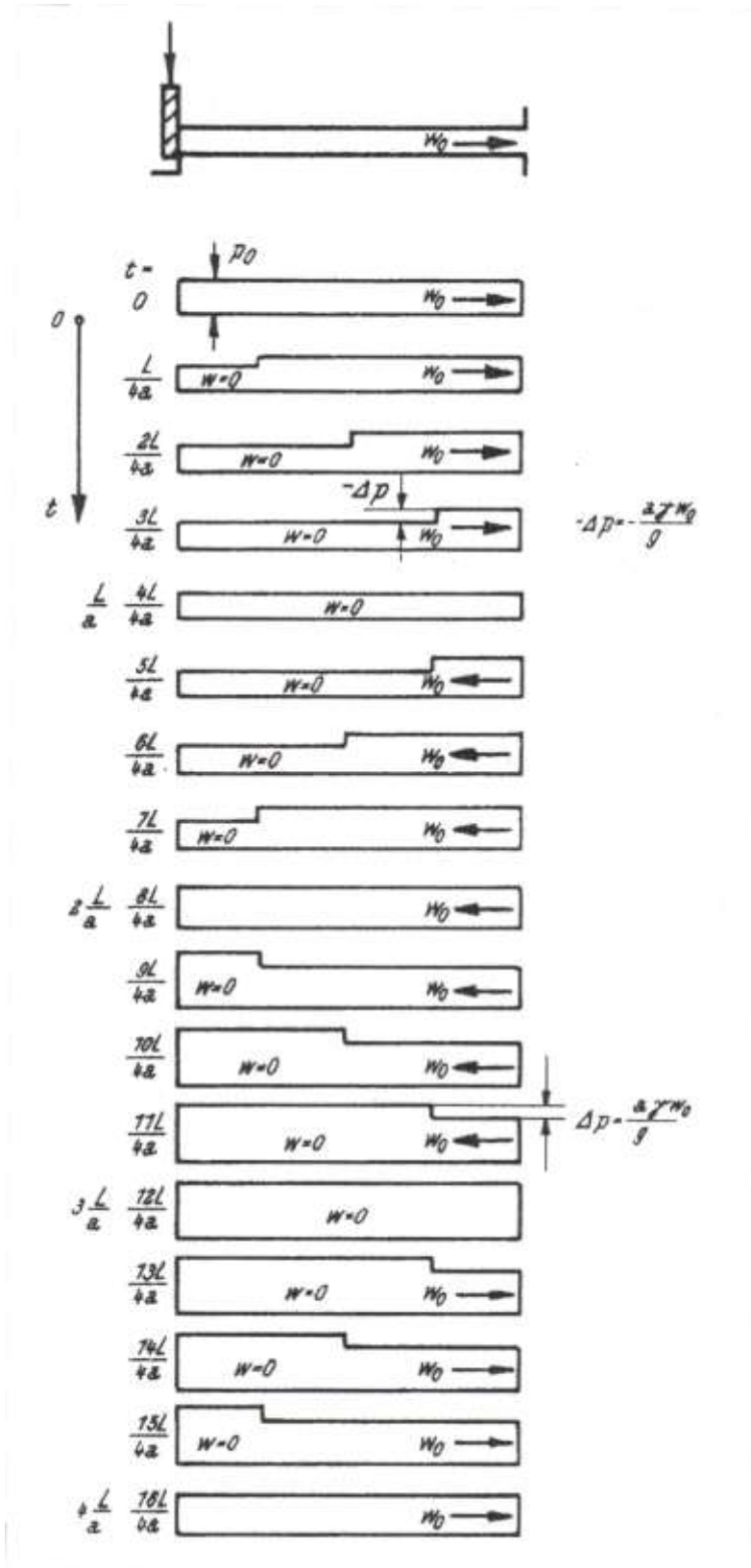


Figure 11: Pressure and velocity sequence behind the valve⁴

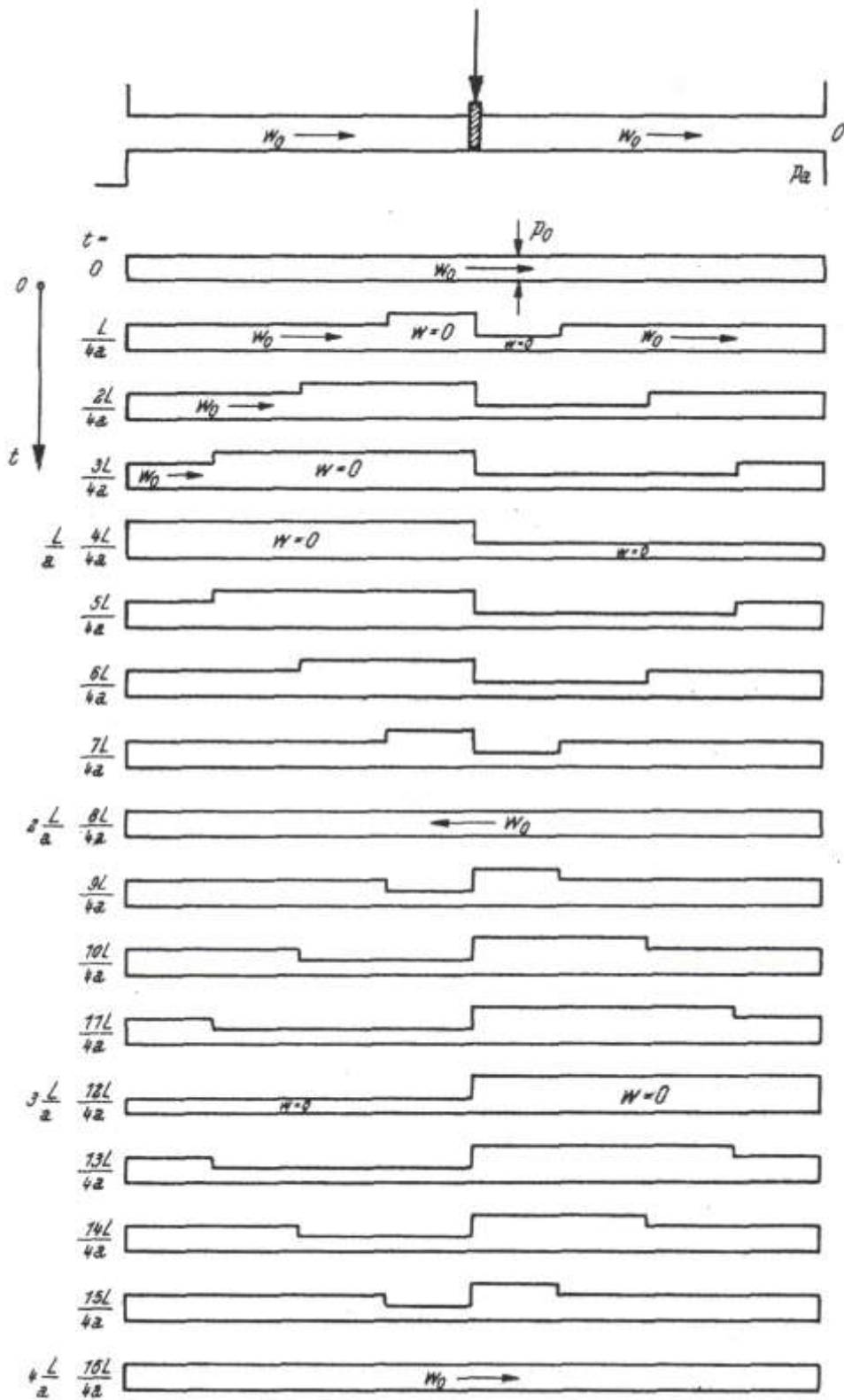


Figure 12: Pressure and velocity distribution along the whole pipe⁴

7.3.3 Speed of Sound Determination

Pressure waves propagate at the speed of sound which is different in each medium. The velocity [m/s] of sound in liquids and gases can be determined by following equation:

$$v = \sqrt{\frac{K}{\rho}} \quad (8^7)$$

where ρ [kg/m³] is the density of the medium and K [N/m²] the compression modulus. For liquids instead of K often the bulk modulus B is used, but the meaning is the same. The compression modulus can easily be explained. It's the ratio between the pressure acting on a medium and its resulting volume change:

$$K = \frac{p}{\Delta V / V} \quad (9^7)$$

The speed of sound in a massive stick, which represents a special case, is determined by replacing the compression modulus K in Equation (8) by Young's modulus E . For a massive stick it is assumed that its diameter is significant smaller than the wave length of sound.

$$v = \sqrt{\frac{E}{\rho}} \quad (10^7)$$

So it can be said that the speed of sound and so pressure wave velocity is dependent on media properties as density and compressibility.

Liquids and solids are relative incompressible, therefore they have higher values for the compression modulus which is rather independent of temperature and pressure. However, gases are strongly compressible and their K -values are much smaller and highly dependent on temperature and pressure.

The reciprocal of the compression modulus is the compressibility:

$$\kappa = \frac{1}{K} = -\frac{\Delta V / V}{p} \quad (11^7)$$

Equation (8) explains mathematically why the speed of sound in air is lower as it is in steel, for example. A higher denominator delivers a higher velocity. In the table below values for certain media are listed. These values are from experimental series only and therefore cannot be seen as exact. Looking up these values one gets a different value for each literature source.

Air (20°C)	343 m/s
Helium	981 m/s
Water	1484 m/s
Ice (-4°C)	1402 m/s
Oil	1740 m/s
Wood	3300 m/s
Iron	5170 m/s
Steel	5920 m/s
Aluminium	6300 m/s
Diamond	18.000 m/s

Table 1: Speed of sound in different mediums⁸

The range in the table can also be explained easily from the physical side. The speed of sound is determined by the elasticity and density of the specific medium. Generally can be said that each medium is somehow compressible, otherwise it would immediately decompose if any impulse is acting on it. Pressure waves propagate through atoms or molecules and they oscillate around their neutral position, which is a state of equilibrium⁷. What propagates is not the medium itself, but the state of movement of the molecules. This state is described by energy and impulse. Energy and impulse are transferred by the molecules as they bump against each other. In steel molecules are arranged very close to each other in a rigid crystalline structure. Any movement or change of the crystalline structure would afford high quantities of energy. So the energy, which faces the molecules, is immediately transferred to its neighbors. The short distance between the molecules and their stable arrangement are responsible for the high propagation velocity and rather small energy losses.

Derivation of pressure wave velocity equation

A horizontal pipe filled with fluid of certain density is considered. Figure 13 illustrates the device.

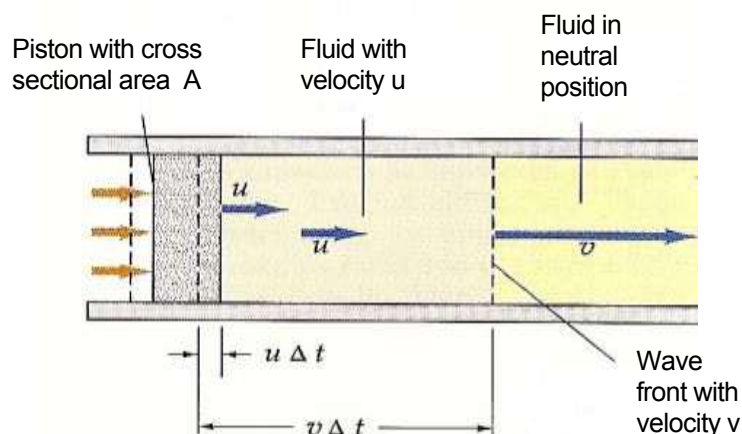


Figure 13: Piston in a liquid filled pipe⁷

The pipe includes a piston with a cross-sectional area A . For a short moment (Δt) the piston is moved to the right which results in a fluid density increase at that point. The

pressure at the left end of the liquid column increases for Δp . What happens is that the piston hits the molecules of the fluid and they transmit the bump to their neighboring molecules and so a density disturbance propagates along the pipe.

Simplifying it is assumed that during Δt , the piston moves with a constant velocity u and transfers its velocity to the whole amount of liquid. Further more it is supposed that u is much smaller than the propagation velocity v of the generated pressure wave.

In the time interval Δt the piston moves a distance of $\Delta t \cdot u$ to the right and the pressure wave a distance of $\Delta t \cdot v$. That means that at Δt the pressure wave is $\Delta t \cdot v$ in front of the piston. The assumption that the whole amount of liquid at this distance moves with the same velocity u , means that we have a rectangular form of the wave. The speed of sound can now be calculated if the impulse change of the fluid is compared with the acting force F caused by the pressure at Δt ⁷:

$$\text{Impulse} = F \cdot \Delta t = A \cdot \Delta p \cdot \Delta t \text{ [kg m/s]} \quad (12^7)$$

According the second Newtonian axiom $F=dp/dt$, the impulse is equal the total impulse change during a time interval Δt ⁹.

The mass m of the moved amount of liquid is the product of its density ρ and the volume $A \cdot v \cdot \Delta t$. Therefore the impulse change can be defined as following:

$$\text{Impulse Change} = \rho \cdot (A \cdot v \cdot \Delta t) \cdot u \quad (13^7)$$

$$A \cdot \Delta p \cdot \Delta t = \rho \cdot (A \cdot v \cdot \Delta t) \cdot u \quad (14^7)$$

$$\text{or: } \Delta p = \rho \cdot v \cdot u \quad (15^7)$$

Equation (15) is similar to the Joukowsky formula^{4,6} where v is displaced by Δv . The Joukowsky formula is introduced in a separate chapter.

An increase in pressure leads to a compression of the liquid volume. This relation is expressed by Equation (16). Since compression leads to a reduction of the initial volume ΔV is termed negative:

$$\Delta p = K \frac{-\Delta V}{V} \quad (16^7)$$

Before the piston is acting the liquid volume is defined by $V=A \cdot v \cdot \Delta t$. Due to the piston movement the volume is changed by $\Delta V= -A \cdot u \cdot \Delta t$, therefore following is valid:

$$\frac{-\Delta V}{V} = \frac{Au\Delta t}{Av\Delta t} = \frac{u}{v} \quad (17^7)$$

and

$$\Delta p = \frac{Ku}{v} \quad (18^7)$$

using Equation (15) results in:

$$\frac{Ku}{v} = \rho v u \quad (19^7)$$

or:

$$v = \sqrt{\frac{K}{\rho}} \quad (20^7)$$

that is equal to Equation (8).

7.3.4 Dampening of the pressure waves

If a pressure wave is monitored it can be observed that the amplitude of the wave gets smaller and smaller with time and distance. Later in this thesis several simulation runs are documented, where this effect can be recognized. The decreasing of the wave amplitude can have several reasons, which act together.

Dampening of the pressure waves is caused by:

- Friction losses
- Deformation
- Interference
- Shut-in-time > Reflection-time

Friction losses occur at the phase border of fluid and pipe wall and are increased with the inner pipe roughness and any inner surface changes. A second inhibiting force which is acting is the inner friction. It is an energy consumption that occurs as the atoms and molecules of a medium move against each other. The inner friction is responsible for the viscosity of a fluid. For a fluid particle the external forces as pressure, friction and inertia have to be in equilibrium if the system is not accelerated¹⁰.

Deformation can be a further reason of decreasing wave intensity. It is meant that the system, in which the pressure wave propagates, yields. For example, if a pipe expands and the internal diameter increases. The situation is a bit different if the deformation is elastic (reversible), because any movement back to the initial state acts like a driving force. In any case the pipe absorbs kinetic energy.

Shut-in time and reflection time are two important parameters for water-hammer calculation. As already mentioned if the shut-in time is very short, the pressure acting on the valve is higher as it would be in case of a slower closing. The highest pressure in the system is obtained, if the shut-in time is smaller than the reflection time. This is not the case if the valve closing lasts several seconds for instance. So if the cross sectional area of a valve is decreased slowly smaller pressure waves are generated continuously as long as the fluid flows. This leads to an overlapping of generated and reflected waves. This phenomenon is called interference. It is distinguished between constructive interference and destructive interference. Constructive interference occurs if two sinus waves with same length, phase and frequency overlap. This would lead to an increase of the amplitude of the final wave. If the waves have the same amplitude but a phase difference of 180°, which means that a wave trough meets a wave valley, they discharge each other^{4,7}.

The shape of the pressure peak is dependent on the shut-in time, on friction forces along the pipe and on the pressure-loss coefficient of the valve. During the closing process, the highest pressure increase is generated within the last 20% of closing⁴. A valve, for example, which is closed in 2 seconds will cause most of the pressure pulse in the last 0,4 second. In Figure 14 pressures vs. shut-in time is plotted. The longer it takes to close a valve the slower the pressure will increase.

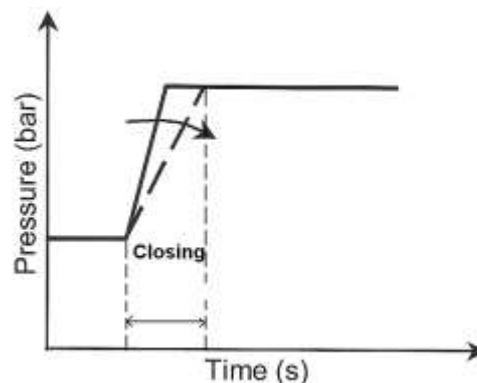


Figure 14: Water hammer measured on a quick-acting valve

7.4 Transients in Horizontal Pipes

Before applying the information above in combination to the 16" casing cementation, let's take first a closer look to the pressure behavior in horizontal pipe systems.

As a quick acting valve in a pipeline is operated, a pressure pulse will be generated. The pressure wave will propagate both up-stream and down-stream of the valve. The magnitude of such a pressure pulse can be calculated by Joukowsky formula which is only valid if the shut in time is shorter then the reflection time. The reflection time is the time the pressure wave takes for twice the distance to the point where it is reflected. That means the valve has to be closed before the generated pressure wave returns again at the valve after it was reflected.

If the closing takes longer Δp is reduced due to wave overlapping. This overlapping would be created if the reflected pressure wave meets those waves which are generated continuously at the decreasing cross sectional area of a pipe as the valve closes.

Joukowsky formula for water hammer calculation:

$$\Delta p = \rho a \Delta u \quad (21^4)$$

where ρ (kg/m³) is the fluid density, Δu (m/s) the fluid velocity change and a (m/s) the speed of sound in the fluid. In other literatures often c (celerity) is used instead of a . Since the fluid velocity is decreased to zero Δu is equal to the steady state velocity. If a pressure wave propagates through a piping system the pipe properties have a significant influence on the magnitude of the pressure peak. As already mentioned pipes tend to enlarge in diameter as a water hammer effect occurs. This fact is not unimportant as it influences the wave speed. Up to now Equation (8) to determine the speed of sound was introduced. In order to consider Youngs modulus, diameter and wall thickness of a pipe, following equation is used:

$$a = \frac{\sqrt{\frac{1}{\rho_F}}}{\sqrt{\frac{1}{E_F} + \frac{D}{t + E_P}}} \quad (22^4)$$

where

E_F = the bulk modulus of the fluid media,

E_P = Youngs modulus of the pipe (2,1e11 N/m²),

D = inner diameter of the pipe,

t = pipe wall thickness,

ρ_F = fluid density.

Water-Hammer-Example

Assuming water is flowing with 0,5m/s through a horizontal 100m long pipe with an internal diameter of 300mm and a wall thickness of 20mm.

After quickly closing the valve the Joukowsky pressure peak can be calculated by applying Equations (21) and (22).

$$a = \frac{\sqrt{\frac{1}{1000}}}{\sqrt{\frac{1}{2,1e+9} + \frac{0,3}{0,02 + 2,1e+11}}} = 1350 \text{ m/s}$$

$$\Delta p = 1000 \cdot 0,5 \cdot 1350 = 6,76 \text{ bar}$$

The resulting pressure increase after Joukowsky is 6,76bar. As already mentioned this calculation is only valid if the valve shut in time is shorter than the pressure wave reflection time.

This example was also run with a simulation software and the results are illustrated in Figures 15 to 17. From Figure 15 it can be seen that the calculated and simulated value of Δp correspond well. The liquid source is a water bond with a liquid level of 100m, which is similar to a pump pressure of 9,81bar. This can be seen from the steady state condition within the first five seconds. The pressure measurement was directly taken at the valve which has the same cross sectional area as the pipe. In the simulation the valve is closed after 5 seconds of continuous flow within in 0,01 seconds. Since the speed of sound in water is about 1480m/s, the pressure wave takes 0,067 seconds for one distance. The reflection time is the time the wave needs for one time back and forth. Therefore the valve has to be closed within 0,135 seconds, otherwise the Joukowsky formula would not be valid.

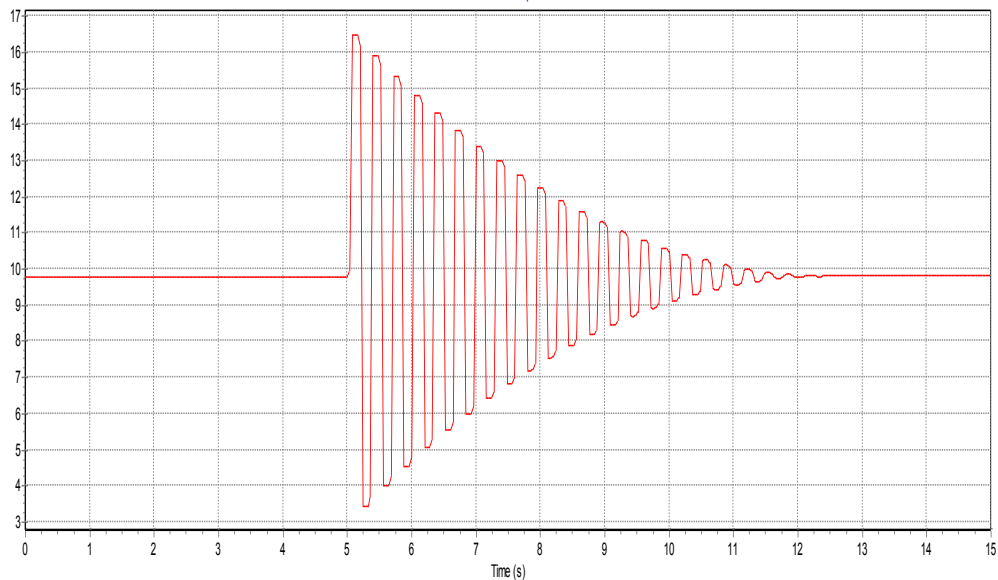


Figure 15: Pressure sequence caused by water hammer in horizontal pipe

In Figure 16 the pressure drop behind the valve is shown. As soon as the fluid flow is interrupted the inertia of the water forces the liquid to flow a bit further and not to stop immediately. A suction effect arises and a negative pressure wave is generated. A pressure wave is termed to be positive if its magnitude is above steady state conditions. They are generated in front of a closing valve. Negative transients appear first after a closing valve and their magnitude is lower as the steady state pressure within a system.

The Δp of the first pressure peak in Figure 15 and Figure 16 have the same value. If for example the inner diameter of the pipe section behind the valve is smaller, the Δp in Figure 16 would be higher since the fluid velocity would be increased in a smaller cross-sectional area. This will be relevant for the simulation of the 16" casing string within the 20,4in (average value of caliper measurement) borehole.

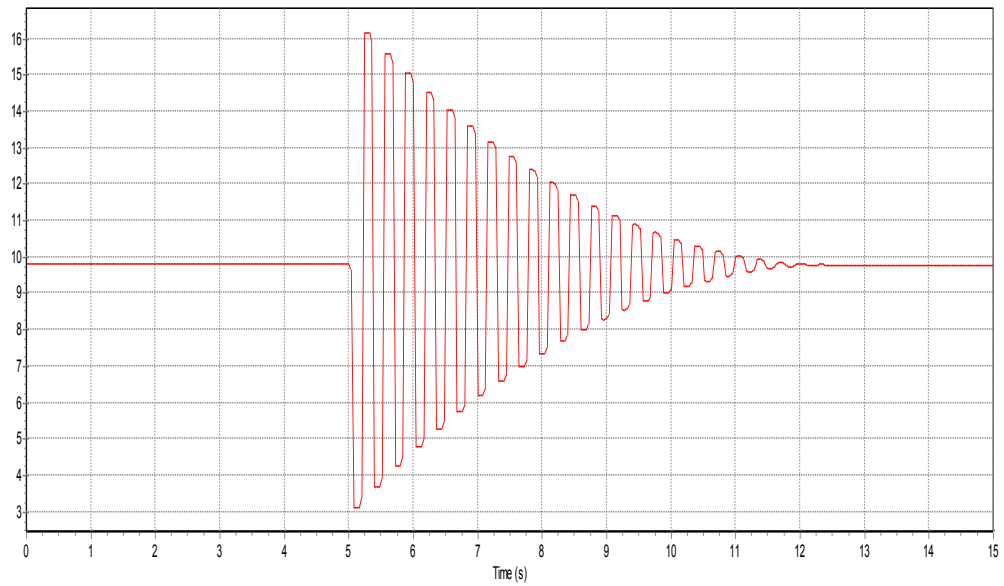


Figure 16: Water hammer effect behind the valve

Figure 17 illustrates the total pressure change across the valve. This means the difference between the positive pressure wave before the valve and the negative after, or in other words the sum of the two Δp . Therefore the graph shows 0 pressure change for the steady state condition in the first five seconds.

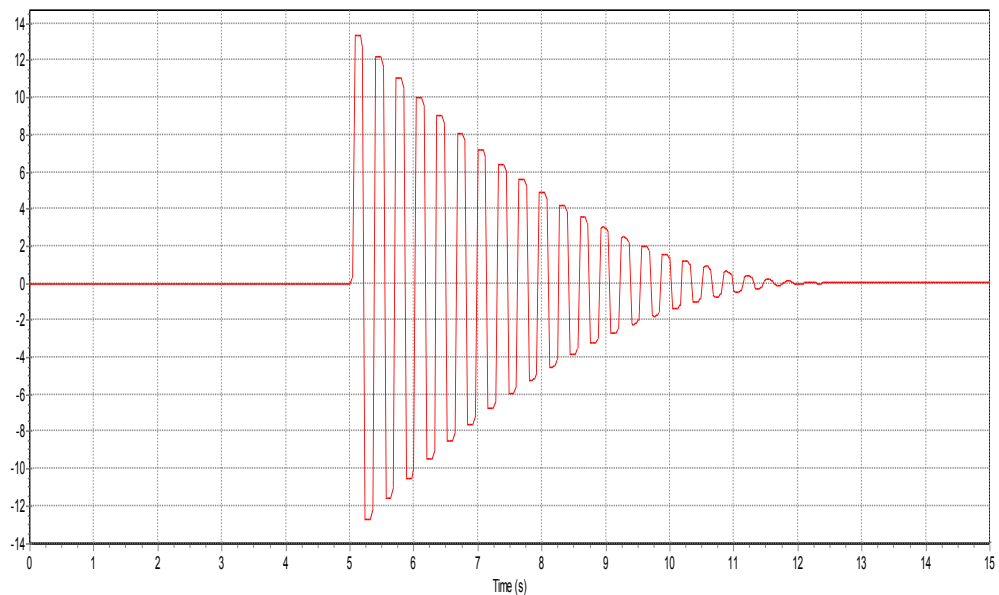


Figure 17: Total pressure across the valve

7.5 Transients in Vertical Pipes

In order to investigate the possible water hammer effect at the 16" casing string the difference between a water hammer in a horizontal and in a vertical pipe has to be ascertained. The example of the previous chapter is now simulated with a vertical pipe using the same boundary conditions. Water is flowing at a speed of 0,5m/s through a 100m vertical pipe with an inner diameter of 300mm and a wall thickness of 20mm. Again the water source is a bond on top of the pipe with a liquid level of 100m. The results are presented in Figures 18 to 20. It can be clearly seen that in steady state conditions the pressure at the valve is about 19,6bar. This is the sum of the hydrostatic pressure in the

100m vertical pipe and the hydrostatics the 100m water level in the bond or in other words a pump pressure. The following three figures illustrate the pressure behaviour determined directly before and after the valve and the total pressure change across the valve.

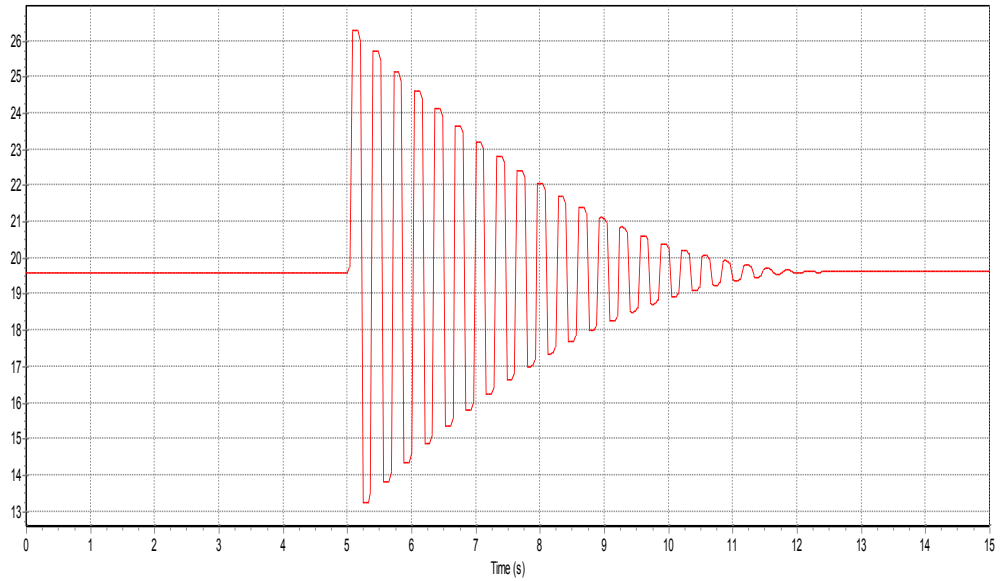


Figure 18: Pressure sequence at the valve, simulated in vertical pipe

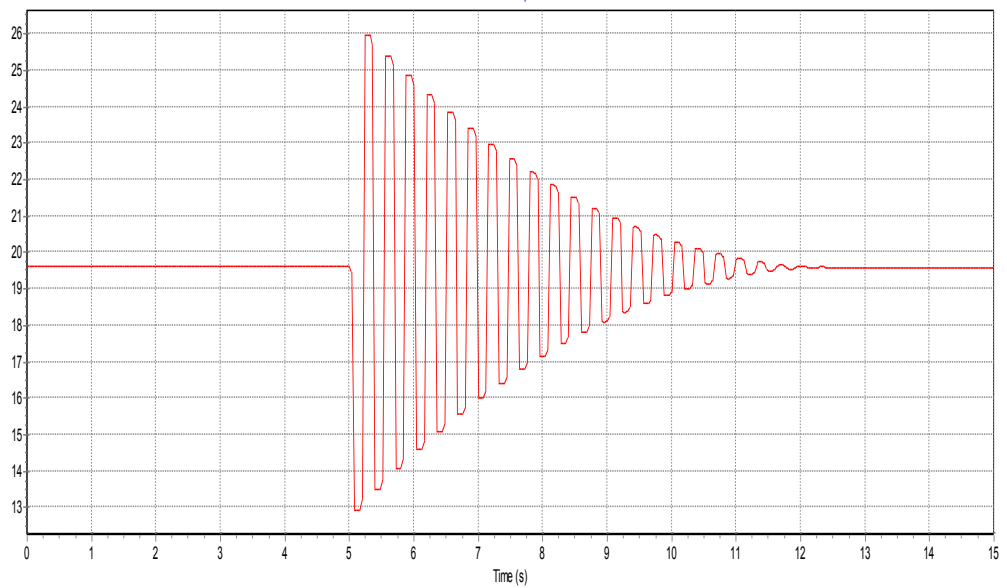


Figure 19: Pressure sequence behind the valve, simulated in vertical pipe

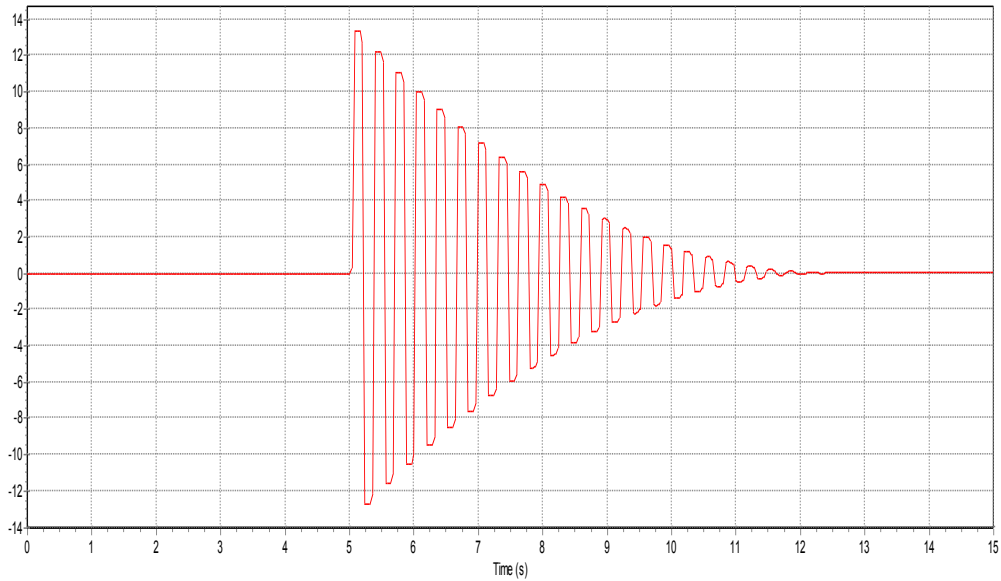


Figure 20: Total pressure across the valve in vertical pipe

The simulation shows that the difference between the pressure peak in a horizontal pipe and in a vertical pipe is the hydrostatic pressure, in this case 9,81bar. Another interesting aspect is that even in a vertical pipe the magnitude of a negative pressure wave (Figure 19) behind the valve is not affected by the hydrostatic pressure. Therefore the total pressure difference is the same in both cases.

The reason for choosing a higher inlet pressure as it would be necessary for achieving a fluid velocity of 0,5m/s, is that the simulation program has problems with the pressure calculation if the pressure drops below the vaporisation pressure which is 0,017bar for water. This phenomenon is called cavitation and results in forming “gas pockets”.

7.6 Measuring of Pressure Waves

In the Figure 21 a typical set-up for a pressure pulse experiment is shown. The fluid flows from the left to the right. At time point 0 the pressure in B is higher than in A otherwise no fluid flow can be generated. It shows a quick-acting valve and two pressure transducers, A and B, upstream of the valve. As the quick-acting valve closes, it generates a rapid increase in pipe pressure at A and B. The pressure wave will arrive at A first, than at B. The time difference is defined as the time-of-flight. Therefore a set-up like this can be used to determine the speed of sound in any liquid or gas-liquid mixtures.

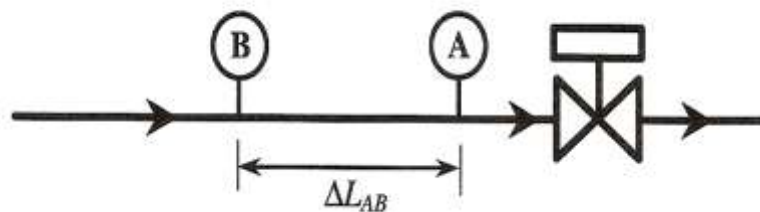


Figure 21: Pressure pulse set up for a pipeline

As speed of sound in water is about 1480m/s, pressure transducers have to be rather sensitive in order to detect those initial pressure values.

8. Water Hammer Simulation

The calculation of a water hammer can also be done with several simulation softwares. This is quite useful, especially if boundary conditions can not be considered that easily. For example if a transfer system contains several phases boundary conditions change with time.

In the previous chapters the task of this thesis and the theoretical background of the water hammer effect were discussed. This chapter guides step by step to a final result of the problem. Remembering the task is to determine the loading present during 16" casing string primary cementing operation.

Further more it will be interesting to compare results out of simulation runs with those calculated by the Joukowsky formula.

The author had the possibility to work with two different software programs called "Fluent 6.3" and "Wanda 3". "Fluent" is one of the most developed programs in computational fluid determination (CFD) therefore it is also a quite complex software. It can be used together with "Gambit", "CAD" or "SolidWorks", which are design programs that produce the geometry of a problem such as pipes, gearboxes or rotors for example. The author became aware of this software since it can be used at the University of the Leoben.

"Wanda 3" is an advanced software product to support the hydraulic design process of pipeline systems and can be used for hydraulic analysis of steady and unsteady flow conditions. "Wanda 3" was developed by "Delft Hydraulics". The author became aware of this program as he found out that for hydroelectric power stations in Austria, the hydraulic engineering design is supported by this software. Therefore it seemed that "Wanda" is quite suitable for determining a water hammer effect considering large dimensions.

All simulation runs using above mentioned programs were performed by the author.

8.1 Simulation with "Fluent"

Simulating with "Fluent" a steady state flow through a pipe delivered the expected result which is shown in Figure 22 and 23. It can be recognized that the fluid velocity at the pipe wall is zero. In Figure 23 the pressure distribution is illustrated. As expected it decreases with length.

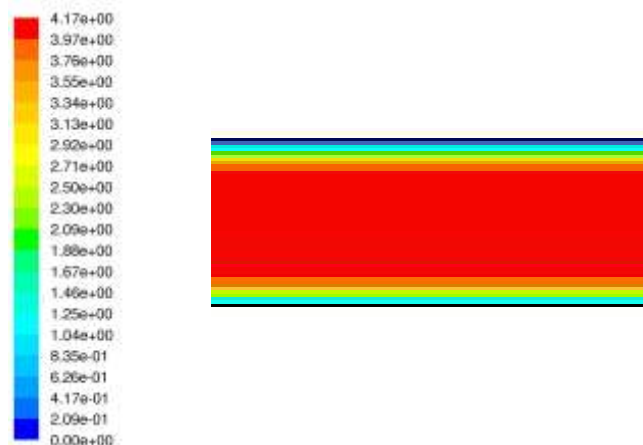


Figure 22: Zoom in of fluid velocity profile in a pipe

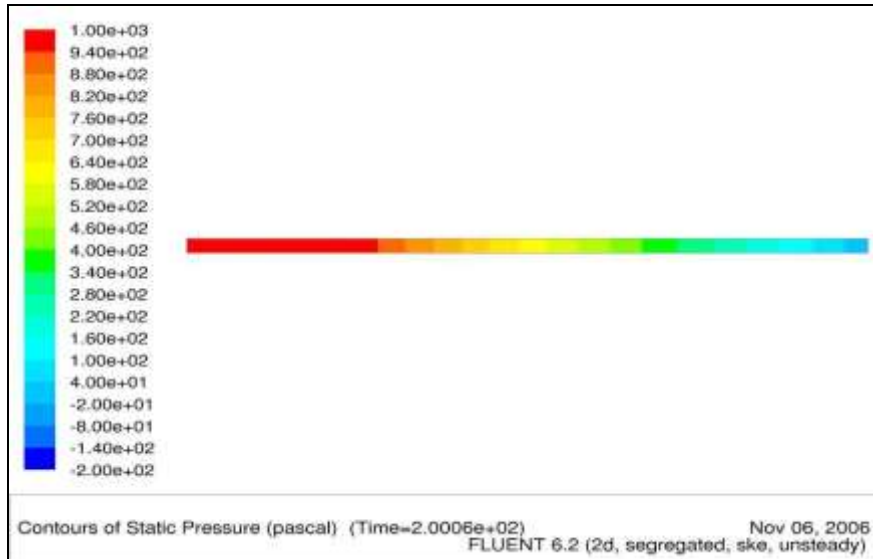


Figure 23: Pressure distribution along the pipe

In order to simulate a water hammer a valve was installed in the middle of the pipe. Introducing the valve into the program turned out to be a little bit complicated. At first the fluid flow has to be determined as an unsteady flow in order to interrupt the iteration process. Interrupting the iteration process is necessary to change the settings of the boundary conditions. The location of the valve is defined as an interface which can be switched from "interior" to "wall". This change let suddenly a wall appear in the middle of the pipe and the iteration process can be continued. What happened is shown in Figures 24 and 25.

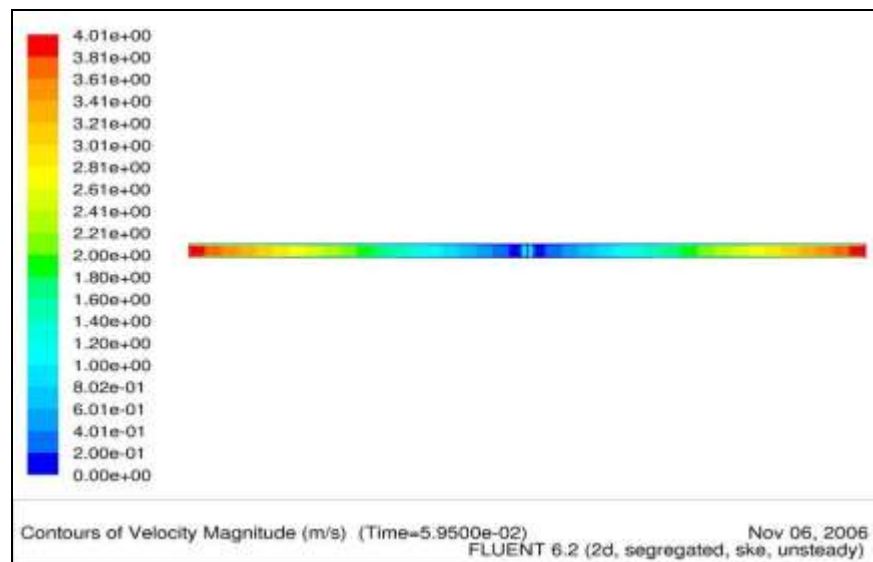


Figure 24: Velocity distribution caused by the water hammer

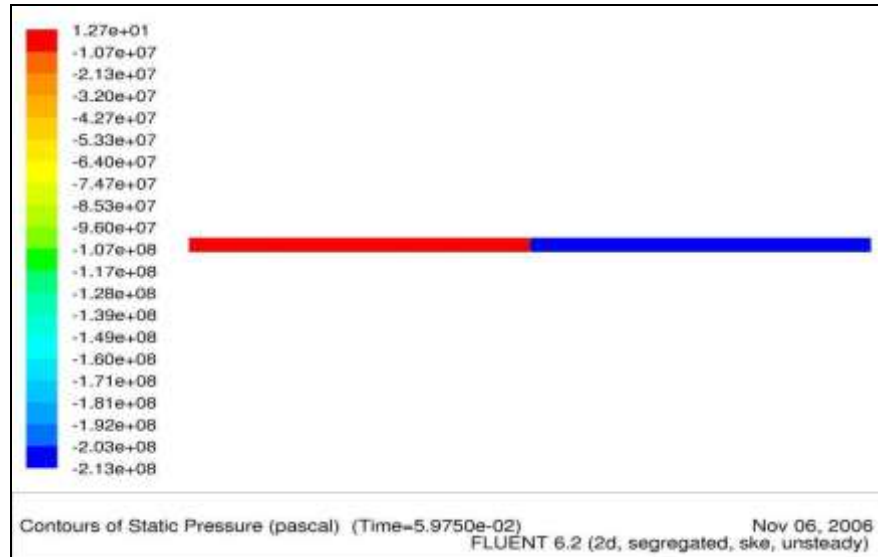


Figure 25: Pressure distribution after valve has closed

In Figure 24 the impact of the suddenly initialized wall on the velocity distribution can be noticed. On the left side the initial velocity of 4m/s at the inlet can be noticed. The fluid flow slows down towards the valve and become zero. Directly at the valve, the two lighter spots at both sides indicate some whirling. It can be seen pretty clear how the fluid flow is “cut” in the middle and forced to slow down, even after the valve.

Concerning the pressure distribution in Figure 25 no pressure wave or any linear change in pressure can be detected. In “Fluent” the user has the possibility to make and save pictures of changes in state of an unsteady process, for instance velocity or pressure changes in a system. The user defines the time interval and the sequence when the pictures are made. At the end of the simulation you have stored so many pictures, that it would be possible to create an animation. In this case the author tried to catch the pressure wave as it propagates from the valve backwards to the inlet. Figure 25 is showing the first picture made but as you can see the pressure distributions in front and after the valve are the same. Although after increasing the sequence of the pictures a pressure wave detection was not possible. Considering the wave takes $6,7 \cdot 10^{-4}$ seconds for one meter, it is not surprisingly that the software cannot picture the wave as occurred. At the scale in Figure 25 a pressure of -2130bar can be read of and lead to an unrealistic and invalid value.

While working with “Fluent” it turned out that the program had big problems in dealing with the sudden interruption of fluid flow due to an appearing wall in the pipe. Most of the time unrealistic results like shown in Figure 25 are delivered. Numerical errors of the program are mainly the cause of these wrong results.

8.2 Simulation with “Wanda 3”

In this chapter the simulation software “Wanda 3” is introduced and its pros and cons from the author’s point of view are discussed.

“Wanda” is a simple and user friendly two dimensional simulation program. A comparison between “Fluent” and “Wanda” does not make sense because they have there advantages in complete different applications. With “Fluent” which can be applied for two and three dimensional problems, fluid flow and heat transfer in rather complex geometries can be determined. Above these geometries a grid is laid and single cells are obtained. Fluent is able to calculate geometries which contain up to several millions cells.

“Wanda” can be applied for the calculations in different types of piping systems of any dimension, like fire fighting systems, sewer systems, water distribution networks, industrial plants or hydroelectric power stations. The mathematical model behind is termed “Method

of Characteristic". This method is not discussed in this thesis. In Figure 26 the operating surface of the program is illustrated. It consists of the diagram window, which is the larger one with the white back ground, a hydraulic component window and on the right the component property window. The component window is a kind of data base which contains a large variety of pipes, pumps, valves, bonds etc. By selecting a component from this library and dragging it to the diagram window the user can build a hydraulic model. In the property window the single components are defined. By clicking on any component its property window is opened automatically. In Figure 26 for instance you can see that the pipe in the diagram window is marked and its diameter of 300mm is defined in the property window.

"Wanda" offers two different calculation mode called "Wanda Engineering" and its extension "Wanda Transient". The first one is used for steady state conditions. It can be used for flow and pressure balancing, for the evaluation of flow capacities and pipe diameters or for hydraulic gradient evaluations. "Wanda Transient" enables the user to simulate steady and unsteady flow conditions (water hammer) in networks independent of their size. For several components actions can be specified such as valve closing/opening, changes in pump rates or pressures etc. The effects of changing boundary conditions can be measured and illustrated with animation.

In Figure 26 a simple set up for a water hammer calculation is shown. It consists of two bonds filled with water at different levels in order to create fluid flow from the left to the right. These bonds are connected with two pipes and a valve is placed in-between. A special feature of this program is that the liquid levels of the two bonds stay constant therefore the hydrostatic pressure at the bottom of the first bond can be considered as a constant pump pressure. It can be seen in the diagram window that the graphical solution of hydraulic modeling is rather simple. The valve is closed after 2 seconds and a pressure wave is generated.

The front window of Figure 26 shows a pressure vs. pipe length animation of the marked pipe in the example. The orange line illustrates the actual pressure distribution within the pipe, whereas the blue and green lines indicate the maximum and minimum pressure values along the pipe. Before the valve is operated the orange line is straight and slightly decreasing due to a small pressure difference caused by different liquid levels in the bonds. When the valve is closed a water hammer effect occurs at the valve and the generated pressure front shifts backwards towards the inlet. As already explained in the previous chapter the fluid velocity after (right side) the pressure wave is zero and ahead the initial steady state condition is present. Figure 26 is showing the pressure wave while Figure 27 is showing the velocity distribution at the same moment in time during the simulation run. The initial fluid velocity of 1m/s drops behind the pressure front immediately to zero and this change shifts towards the inlet as the pressure wave propagates. Prior in chapter 5.3.2 theoretically discussed pressure and velocity distributions are confirmed by the simulation. In the Figures 28 to 31 the same procedure as in Figure 26 is again illustrated by a simulation run. In the first window the fluid velocity is displayed which is about 0,4m/s for steady state conditions. This value becomes negative if the flowing direction is reversed due to the unbalanced pressure conditions at the valve or at the pipe inlet. The second window shows the propagation of the transient along the pipe. The third window of each figure shows the pressure vs. time relation at the valve or in other words the pressure change at the left end of the pipe. The first peak is the so called water hammer. The vertical line in this plot, which shifts from the left to the right shows how long it takes for the wave to be reflected.

Concerning pressure or velocity distributions in a pipe the author detected a big disadvantage of "Wanda", namely that it is not possible to illustrate these distributions along a vertical pipe. So in case of vertical pipes no animations can be run. Only at specific points like at valves, pipe inlets or outlets changes in flowing conditions can be displayed.

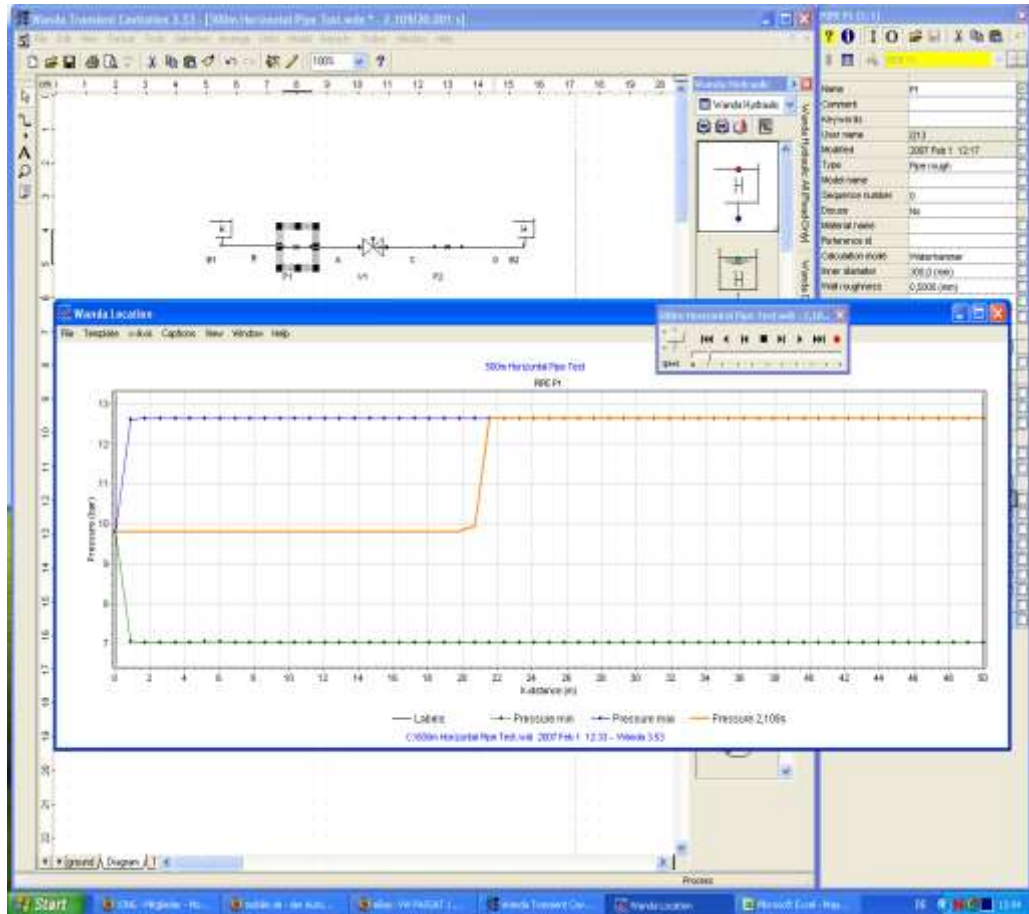


Figure 26: "Wanda" operating windows



Figure 27: Pressure wave causes change in fluid velocity



Figure 28: Pressure wave is generated, fluid still enters pipe



Figure 29: Pressure wave propagates towards the inlet, zero fluid velocity behind the wave front



Figure 30: Wave front has reached inlet, zero fluid velocity along the pipe



Figure 31: Pressure wave was reflected, fluid exits pipe through the inlet

After this introduction to “Wanda 3” the different steps in the determination of the water hammer that probable occurred at the 16” casing string are explained next.

9 Simulation of Water Hammer at MQE-1

One of the greatest challenges during this thesis was to understand and adapt the simulation program “Wanda” to this specific task. “Wanda” was neither developed for multiphase flow nor to simulate cement slurries. All considerations and determination steps are described in this chapter.

9.1 Defining Boundary Conditions

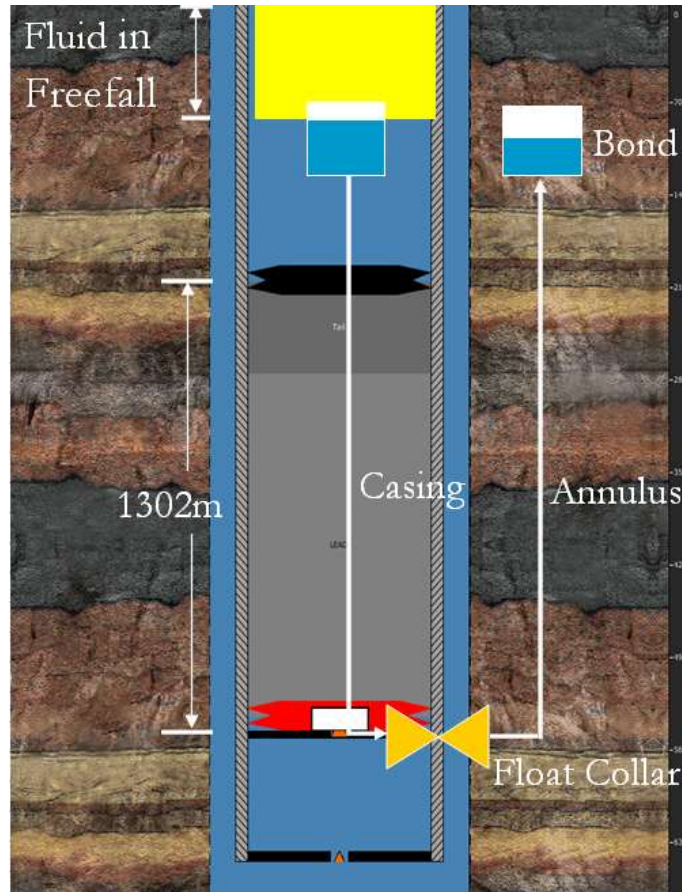


Figure 32: Adaption of the plug cementation to the simulation program

9.1.1 U-Tube

First of all the casing cementation is considered as a U-tube. This is a common comparison for a pipe – annulus configuration and can also be applied in this case (figure 32). The cross sectional area of the second part of the U-tube is equal the cross sectional area of the annulus. For the hole diameter the result of the calibre measurement is used. This is an average value of 519mm (20,43 in). Therefore the inner diameter for the annulus equivalent pipe is 322,8mm (12,7 in):

$$A_{AN} = \frac{\pi}{4} (d_1^2 - d_2^2) = \frac{\pi}{4} (519^2 - 406,4^2) = 81838,5 \text{ mm}^2$$

$$d = \sqrt{\frac{4 \cdot A_{AN}}{\pi}} = 322,8 \text{ mm} = 12,7 \text{ in}$$

9.1.2 Bonds

The bonds on top of the U-tube provide the desired flow rate. Why a bond with a certain liquid level is used instead of a pump has the following reason. If the valve at the bottom is closed and the pump continuously pumps the pressure would increase infinitely and the pressure peak caused by the water hammer could not clearly be defined. Furthermore the situation on site was different because due to the free falling period the pressure at the pump was 0. The free falling phenomenon caused a phase boundary between vapour and liquid (Chapter 6). This boundary condition is defined by the bond where the liquid level is open to the atmosphere. The second bond is necessary because the program requires a kind of vessel at an exit of a pipe. In this case the atmospheric conditions exactly correspond to the conditions on site as the annular return rates face surface conditions.

It was not possible to define exactly the flowing velocity of the cement slurry on its way downhole but cementing engineers suggested from experience a pump rate of 12 bbl/min in this specific case, which means a fluid velocity of 0,3 m/s. Therefore the liquid levels within the tanks on the top of the U-tube were adjusted to provide a fluid velocity of 0,3 m/s. The difference of the liquid levels is 4,6 m and thus this hydrostatic difference between the two pipes provides the flow rate. In "Wanda" the liquid level in the tanks stays constant and so the flow rate is kept constant.

9.1.3 Float Collar

In order to simulate how the cement column is immediately stopped when the bottom plug is landing, the float collar is replaced by a valve with an internal diameter equal to that of the pipe. Although the internal diameter of the float collar is much smaller in reality it is chosen for the simulation this way because the cross sectional area of the bottom plug stopped the fluid column and faced the sudden pressure peak. The suddenly plugged single valve float collar can be compared with a quick closing of a valve because the effect for the cement column above is the same. In the simulation run the valve is closed after five seconds of continuous flow and the closing takes 0.05 seconds.

9.1.4 Free Falling Zone

The free falling phenomenon was already discussed at the beginning of this thesis. It is proved that during the plug cementation of the 16" casing string a free falling period occurred but it can not be said exactly how a pressure wave behaves if it meets such a discontinuous zone. Simulation runs have shown that if a positive pressure wave meets a negative the magnitude of the positive is reduced by Δp between the pressure at steady state conditions and negative pressure wave. This was tested as fluid flow in a pipe was immediately stopped by a closing valve and the pump on the inlet was shut down before the positive pressure wave reached the inlet. So the transient which arrived at the inlet was reduced by the magnitude of the negative transient.

Furthermore it can not be proved if cavitation took place during the free falling period. In this case a simulation across the cavitation zone would not be possible. Together with the authors supervisor it was decided not to take the free falling period into account. This means the simulated casing length is reduced by the free falling height which existed at the time point when the bottom plug landed.

With the support of Halliburton the free falling height could be evaluated. Therefore the plug cementation was simulated with "OptiCem" which is an advanced software program for cementing operation developed by Halliburton. For the certain point in time a free falling height of 345 m was determined. For the simulation this means the fluid column above the float collar consists of 1190,8 m of lead cement, 111,4 m of tail cement and 369,6 m of mud. In Figure 33 the output of "OptiCem" is displayed. The exact value was taken from cement job design report.

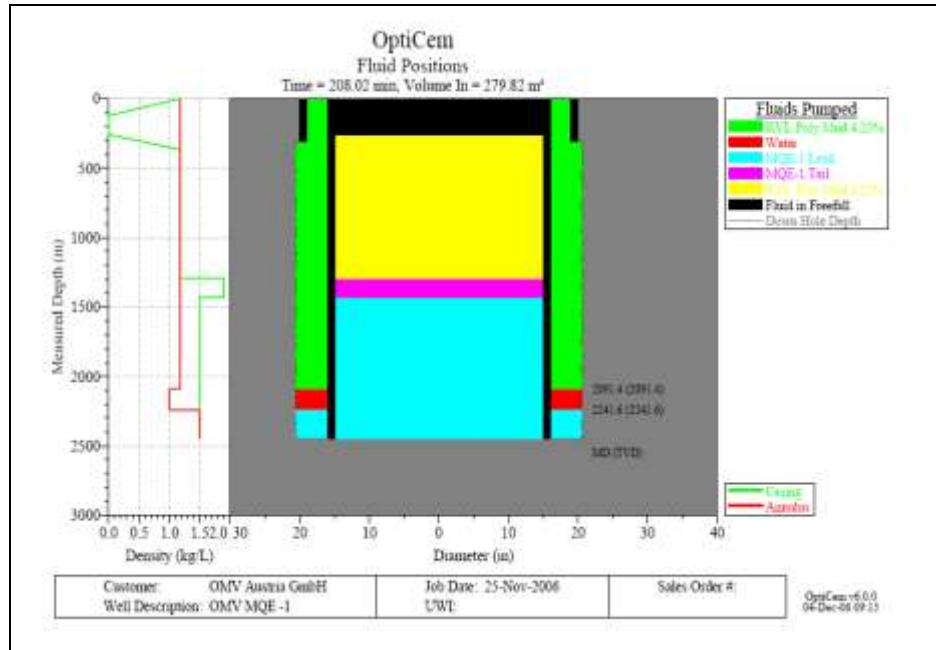


Figure 33: Free falling evaluation with "OptiCem"

9.1.5 Simulation Depth

The casing shoe is situated at a depth of 2440m. As discussed before the free falling length is not considered and therefore subtracted. The float collar is located two casings above the casing shoe at a depth of 2417m. The author decided to take these 23m not into account because they would not influence the magnitude of a pressure wave. The final simulation depth is therefore 2072m.

9.1.6 Different Phases

For a proper simulation the U-tube system is separated into two parts, one before and one after the valve. It is necessary to find out where are the different phases located when the bottom plug is landed. The pumped cement which consists of a lead and a tail slurry is above the bottom plug of course and its column length is about 1302m. Further more the mud which is pumped to displace the cement has to be considered. The free falling phenomenon has an impact on the pumped mud but even when the free falling height is subtracted there is still a mud column of 396,8m left. The previous mud and the spacer have already passed the float collar and are located in the second part of the U-tube. For the application of "Wanda 3" the three phase fluid column above the bottom plug has to be changed into a single phase column. For the determination of the average phase properties the volumetric fraction of each phase is attended. Remembering Joukowski's equation the density plays a significant role for the magnitude of a water hammer.

Density

The volumetric fractions of the different phases are divided up as follows:

$$V_{Mud} = 87,811m^3$$

$$V_{Lead} = 135,945m^3$$

$$V_{Tail} = 21,720m^3$$

$$V_{Total} = 236,47m^3$$

$$F_{Mud} = \frac{87,811}{236,47} = 0,371$$

$$F_{Lead} = \frac{135,945}{236,47} = 0,575$$

$$F_{Tail} = \frac{12,720}{236,47} = 0,053$$

$$Density = 1,18 * 0,371 + 1,89 * 0,053 + 1,5 * 0,575 = 1,4 \frac{kg}{l}$$

Kinematik Viscosity

Another input parameter is the kinematik viscosity which is defined as the dynamic viscosity η divided by the density ρ of a fluid:

$$\nu = \frac{\bar{\eta}}{\rho} = \frac{0,011}{1400} = 7,85 \cdot 10^{-6} \quad (23)$$

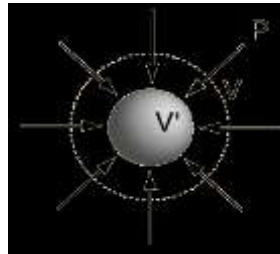
$$[\eta] = \frac{kg}{m * s} = Pa * s = \frac{Ns}{m^2}$$

$$[\nu] = \frac{m^2}{s}$$

In our case the kinematik viscosity was determined with $7,85e-6m^2/s$. The volumetric fraction was also considered for this calculation.

9.1.7 Bulk Modulus

The bulk modulus is a material property and expresses how much it will compress under a given amount of external pressure (Figure 34). It is defined as the ratio of the change in pressure to the fractional volume compression ¹¹. The reciprocal of the bulk modulus is called compressibility



$$B = \frac{\Delta p}{\frac{V' - V}{V}} \quad (24)$$

Figure 34: Fluid compression due to external pressure¹¹

Other moduli describe the material's response (strain) to other kinds of stresses: the shear modulus describes the response to shear, and Young's modulus describes the response to linear strain ¹². For a fluid, only the bulk modulus is meaningful.

The author could neither find a value for the bulk modulus of a cement slurry in literature nor in the industry since in civil engineering Young's modulus of the hardened cement is of importance and not of the slurry. In the following table some values from literature are listed. Liquids with higher values are less compressible. Gases for example have values to the power of 5.

Bulk Modulus	SI Units (Pa, N/m ²) x 10 ⁹
Water	2.15
Seawater	2.35
Mercury	2.85
Glycerine	4.52
Ethyl Alcohol	1.06

Table 2: Bulk modulus of different liquids¹¹

According the advice of Prof. Heigerrth of the Technical University Graz (Austria), the author estimated a value of $2,4e9\text{N/m}^2$ for the bulk modulus of a cement slurry.

9.1.8 Cavitation Pressure

When a volume of liquid faces a sufficiently low pressure the phenomenon of cavitation can be detected. Cavitation describes the creation and decomposition of voids or bubbles due to pressure changes in liquids¹³. Cavitation is usually divided into two classes, the vapour and the gas cavitation. In case of the vapour cavitation the voids contain only little or no gas but vapour of the surrounded liquid. These voids collapse due to the higher external pressure and thereby generate shock waves. In case of gas cavitation the voids are filled with the dissolved gas of the liquid. The voids dissolve slowly since the surrounded liquid starts to diffuse into the gas. General spoken cavitation occurs at fast moving objects in water.

According to Bernulli the pressure in a liquid is lower the higher its velocity. If the fluid velocity is so high that the static pressure drops below the vapour pressure of the liquid, gas and vapour bubbles are developed¹³.

At a plug cementation the inertia of the slurry causes a suction force and thus the pressure drops. For the simulation the cavitation pressure is a further input parameter in order to define the fluid properties. In water cavitation starts at an absolute pressure of 0,017bar and this value is also used for the mud plus cement equivalent phase. It will turn out that this value has no influence on the result of this study because a pressure of 0,017bar is never reached.

9.2 Simulation Execution

After the boundary conditions are defined the simulation can be run. The aim is to receive the magnitude of the water hammer which is the first pressure peak in a pressure vs. time curve measured at the valve. Due to this pressure peak the casing experiences a higher load inside. It has to be considered that this load is further increased since the hydrostatic pressure in the annulus is reduced. In the worst case the casing would burst if the pressure difference across the casing wall exceeded the burst resistance of the pipe (Equation (25)). The reduction of the annular pressure is caused by the inertia of the mud. As soon as the fluid flow is abruptly stopped its inertia forces the fluid to flow a bit further. A suction force is generated which reduces the steady state flowing pressure. This effect causes a negative pressure wave and reduces the annular pressure to even below hydrostatics. This was mentioned at Figure 19.

$$\Delta p_{Burst} = p_{Cas} - p_{Ann}$$

where

p_{Cas} = Pressure inside the casing

p_{Ann} = Pressure in the annulus

Δp_{Burst} = Burst Resistance of Casing

For casing design calculations a safety factor (SF) is considered and the burst resistance (Δp_{Burst}) of a pipe in Equation (26) should not be exceeded by the load acting on the casing, otherwise it is endangered to fail:

$$\Delta p_{Burst} = SF \cdot (p_{Cas} - p_{Ann}) \quad (26)$$

Since for the U-tube simulation the 23m long distance between the float collar and the casing shoe is not taken into account, the valve is located at the deepest point of the U-tube and the pressure measured directly behind the valve corresponds to the pressure in the annulus opposite the float collar. So the sum of the positive Δp and the negative Δp should not exceed the burst resistance of the 16" casing.

If the simulation shows that the burst resistance of the pipe is exceeded, it can be maintained with high reliability that a water hammer effect caused the casing string to fail.

Before the simulation can be started another point has to be marked. The transients are generated in different fluids. One propagates inside the casing where tail, lead and mud are changed into a single phase and the other one in the annulus where spacer and the previous mud are located. This means if the simulation is run with cement equivalent fluid only the magnitude of the positive pressure wave generated before the valve is valid. The value behind the valve would be false as the annulus is filled with a different fluid. In order to get a valid value from behind the valve a second run with the mud equivalent fluid has to be performed. From the second run the measured pressure data behind the valve is used. The different Δp -values of the two runs can only be compared if the boundary conditions stay the same, especially fluid velocity. For the final result the Δp -values of each graph are added and the sum is the total load the casing finally faced. Further when the valve is closed the hydrostatics in the casing and the annulus are different. This fact delivers an additional load to the casing.

It could be seen in the previous pressure vs. time plots of water hammer effects that a certain time period passes by till the valve is suddenly closed and the pressure peaks follow. This time period shows the constant pressure at steady state conditions which is the same before and behind the valve (Figure 18 and 19). It is the hydrostatic pressure of the casing plus the hydrostatic of the liquid level in the bond.

Now in this case the transient graph behind the valve taken from the second simulation run (mud equivalent fluid) will show a much lower pressure during the steady state conditions as the pressure graph taken from the first run (cement equivalent fluid) before the valve. This was expected because the annular fluid has a lower density as the slurry inside the casing. As long as the system is open to both sides U-tube is still acting. At the point of time when the valve is closed two separated systems had to be considered. The hydrostatic in the annulus is less than inside the casing and this difference is the main load on the casing after the displacement process.

The reason why the casing and the annulus in this U-tube simulation are considered as two different systems can be explained easily. First of all it is the only way to simulate the different phases with a one phase simulation program. Further more the mud equivalent fluid in the annulus has no contact to the cement equivalent fluid inside the casing when the water hammer happens.

The two annular fluids have to be changed into a single phase. The density difference between the mud (1,1kg/l) and the spacer (1,0kg/l) in the annulus is not so significant that the author decided not to consider the spacer. If the spacer would be considered and with

the properties of the mud and the spacer a new single phase would be increased slightly compared to the mud and the delta hydrostatic pressure would be slightly reduced. This would lead to a minimum reduction of the pressure wave magnitude. This can be proved by applying the Joukowsky formula. For this calculation a result which might be one bar higher is less critical than one which is lower.

In the following the simulation input data and the results are demonstrated. In Figure 35 the fluid properties windows in “Wanda” are shown, on the left the cement equivalent fluid, on the right the mud equivalent fluid:

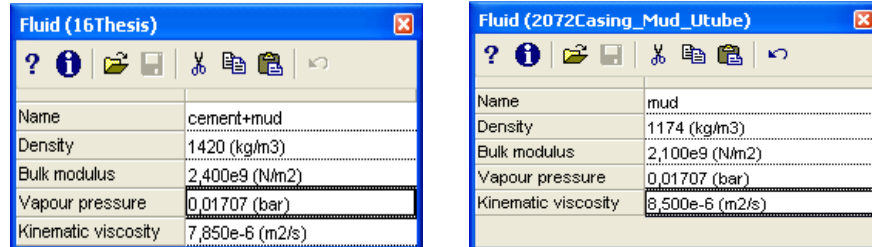


Figure 35: Fluid properties windows, casing fluid on the left, annular fluid on the right

In Figure 36 the input data windows for the U-tube components casing (P1), “annular” pipe (P3) and valve (V1) are shown. The white cells are the input fields and those with the light blue back ground are the output ones.

The wall roughness for the “annular” pipe (10mm) is chosen as high as the program allows. At the input cell “local losses Xi” “TABLE” stands for a hidden input array where local pressure losses caused by changes in flow direction can be defined. In reality the mud is forced to turn its flow 180 degrees after the casing shoe. In the simulated version the 23m between float collar and casing shoe are not considered therefore the 180 degrees turn is defined after the valve.

The output data show the minimum and maximum values that were calculated by the program. Concerning the fluid velocity 0,5m/s instead of 0,3m/s can be read off. The reason is that Figure 36 is a screen shot from a further simulation run where the fluid velocity was increased to 0,5m/s. This further run with increased fluid velocity was performed because the 12bbl/gal (=3m/s) free falling velocity were a rough estimation from the industry.

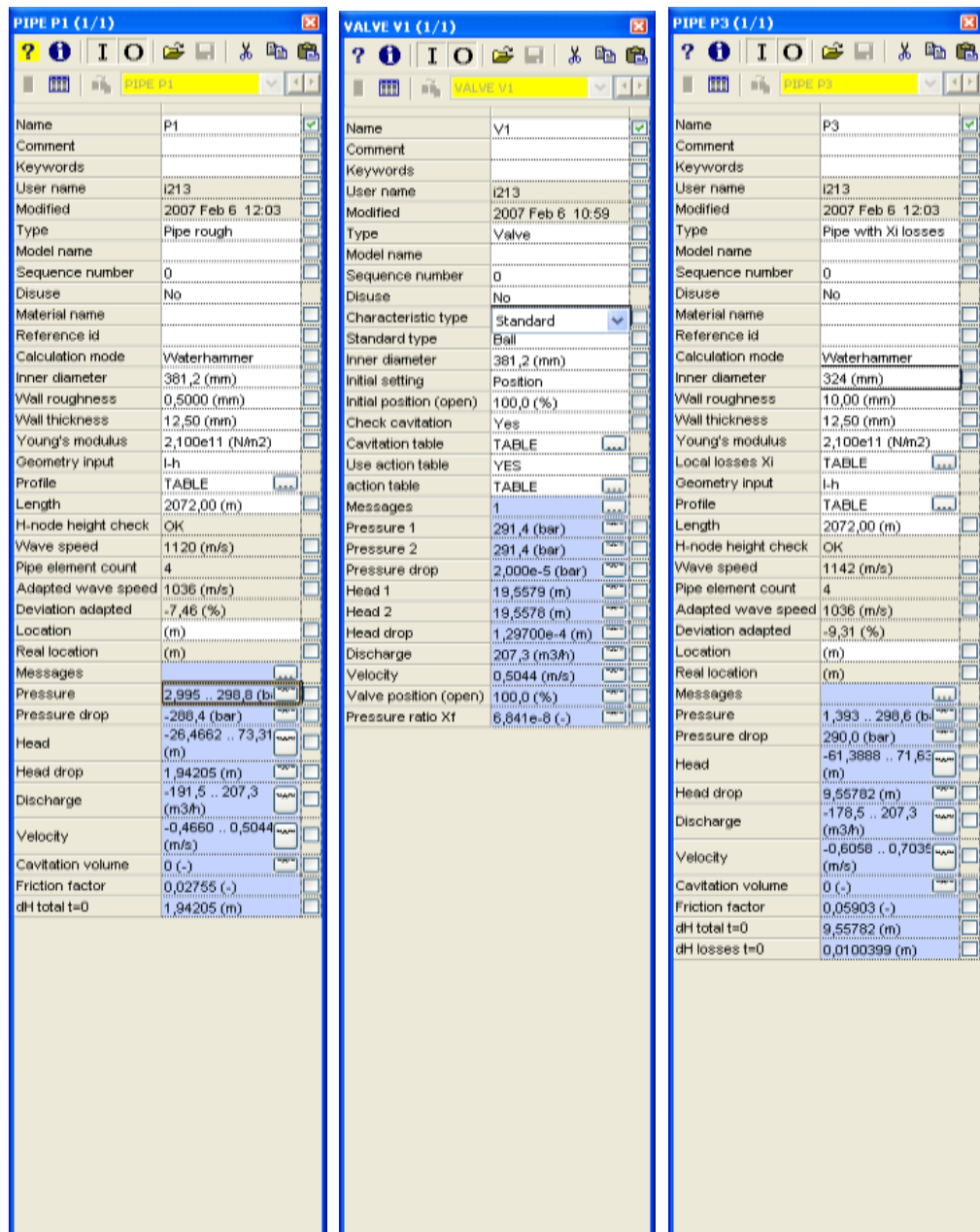


Figure 36: Input Panel for pipe and valve properties

9.3 Simulation Results

The magnitude of the water hammer which probably occurred at OMV's well is illustrated in Figure 37. The first pressure peak is up to 295,74bar and the Δp is 5,17bar. Applying Joukowsky formula and Equation (22) a Δp of 4,7bar is determined. Similar results are obtained by the simulation and the empirical calculation.

After about 80 seconds the pressure wave shows a stable deviation of +/-0,5bar. This behaviour was not expected and could also not be detected at former simulation runs where much smaller pipes were tested. A probable explanation is that due to the large pipe diameter and the inner friction of the fluid a complete reduction of the pressure wave magnitude is not determined by the program.

At the peak itself a linear further pressure increase can be detected during the first 40 seconds, afterwards this increase changes to a decrease. This effect is caused by friction and will be discussed in the following chapter.

In "Wanda" it is possible to copy the calculated data into Excel spread sheets. This has the advantage that several pressure curves can be overlaid or the scale can be changed as it is done in Figure 38.

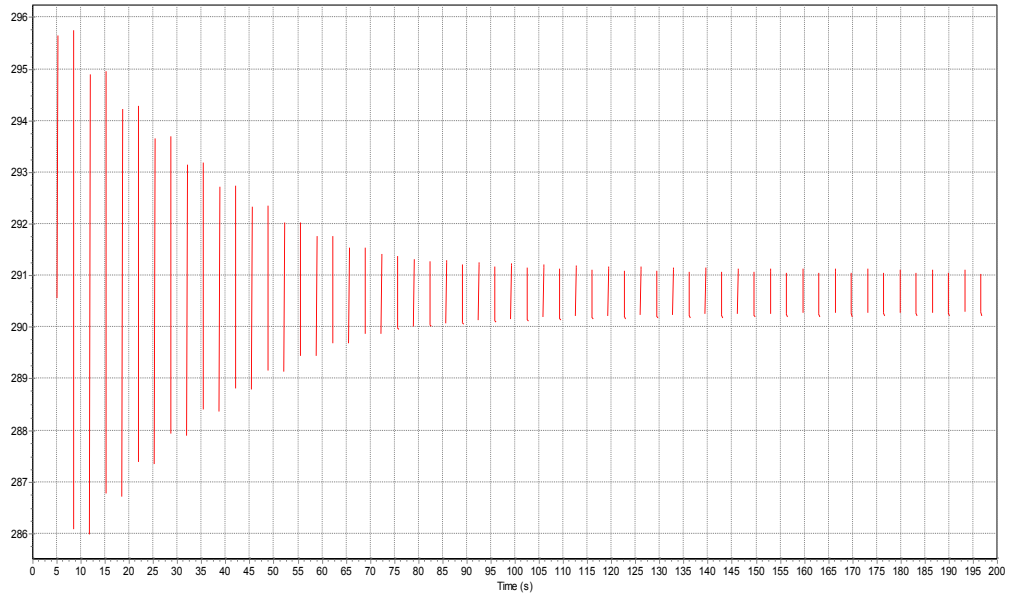


Figure 37: Water hammer effect calculated by "Wanda"

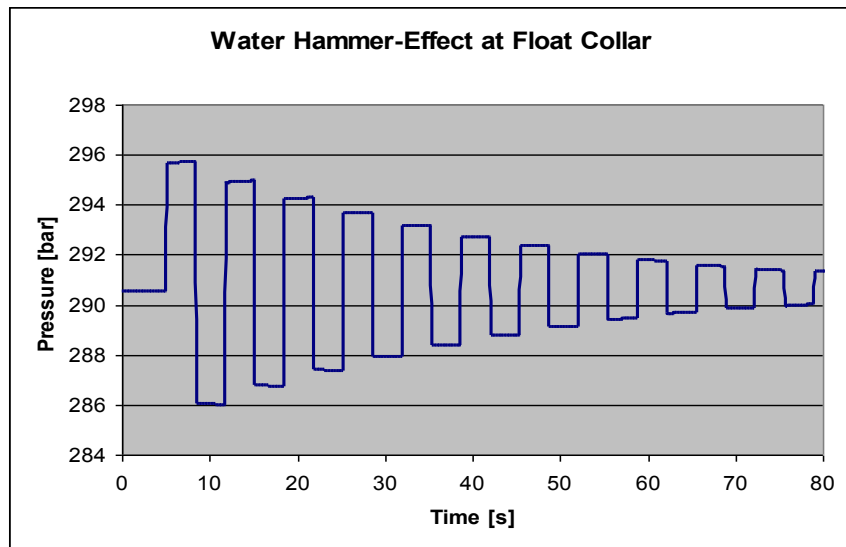


Figure 38: Pressure data transferred into Excel

The effect behind the float collar is illustrated in Figure 39. The 240,23bar correspond to the hydrostatic pressure in the annulus. The first negative pressure peak reduces the steady state pressure by 6bar. After 80 seconds the amplitude is decreased to zero.

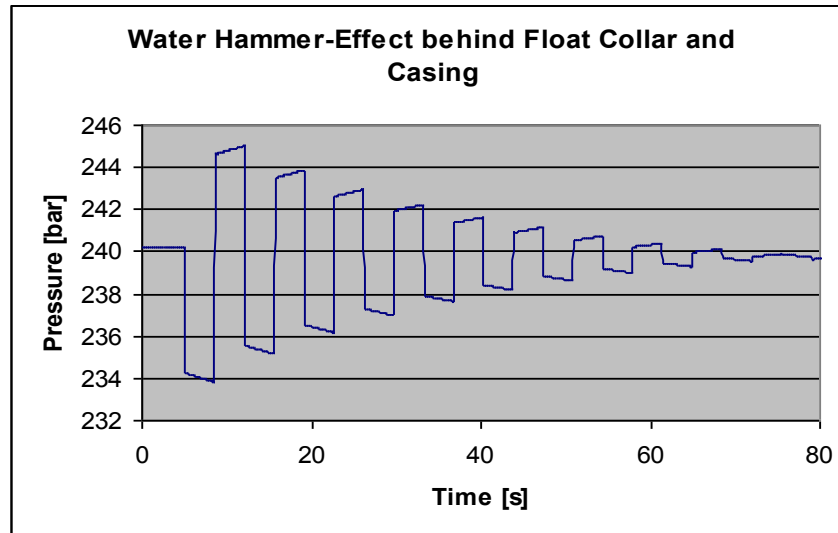


Figure 39: Water hammer effect behind the valve causes a negative pressure wave first

The maximum load the casing faced at the float collar is the sum of the two Δp plus the hydrostatic difference between casing and annulus. Since the valve is closed the casing and the annulus are two different systems with different hydrostatic. The maximum load is determined as follows:

$$\Delta p_{hydr.} = p_{Chydr.} - p_{Ahydr.} = 290,56 - 240,23 = 50,33bar$$

$$\Delta p_{WH} = \Delta p_C + \Delta p_A = 5,2 + 6 = 11,2bar$$

$$\Delta p_{Total} = 50,33 + 11,2 = 61,53bar$$

where:

$p_{Chydr.}$ = hydrostatic pressure in casing

$p_{Ahydr.}$ = hydrostatic pressure in annulus

$\Delta p_{hydr.}$ = hydrostatic pressure difference between casing and annulus

Δp_{WH} = load due to water hammer-effect

Δp_C = load due to water hammer-effect inside casing

Δp_A = load due to water hammer-effect in annulus

Δp_{Total} = total pressure difference

It is obvious that 61,53bar would not cause any harm to pipe body with a burst resistance of 298,5bar¹⁴. The major load is caused by the density difference between the cement equivalent fluid inside the casing and the mud equivalent fluid in the annulus. This load stays constant whereas the 11,2bar of the water hammer-effect decrease with time. In Figure 40 the pressure wave sequences in the casing (blue line) and in the annulus (red line) are plotted. The amplitudes of the pressure waves decrease with time and the hydrostatic pressure difference between casing and annulus is left. If the annulus and the casing would contain the same fluid the two curves would meet again after a certain time.

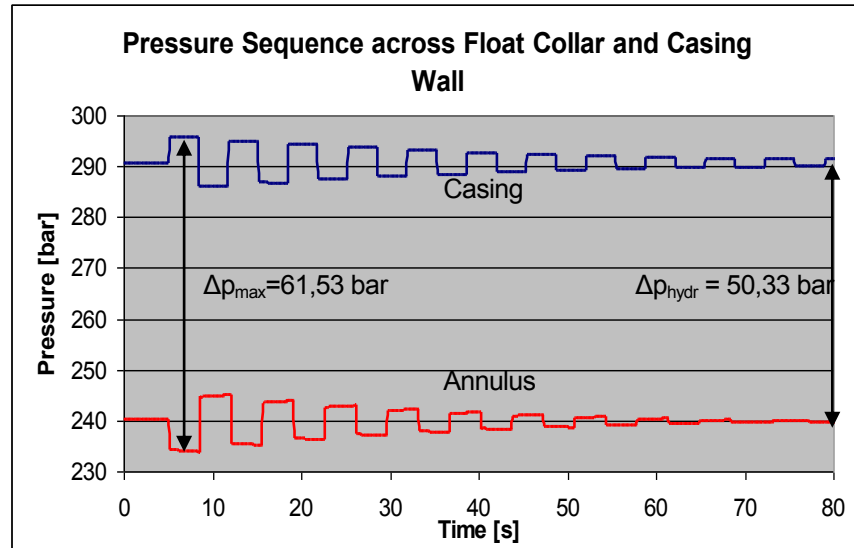


Figure 40: Load at the casing

In Figure 41 the two amplitude curves of the water hammer are plotted and overlapped on a Δp -scale. Hydrostatic is not considered in this plot, only the impact of the water hammer to the pipe is shown. The magnitude of the first pressure peak of the blue line differs from that of the yellow. This leads back to the smaller cross-sectional area of the annulus compared to the casing. The black curves connect the peaks and the difference between these two curves is an approximation of the load only caused by the water hammer-effect across the casing wall.

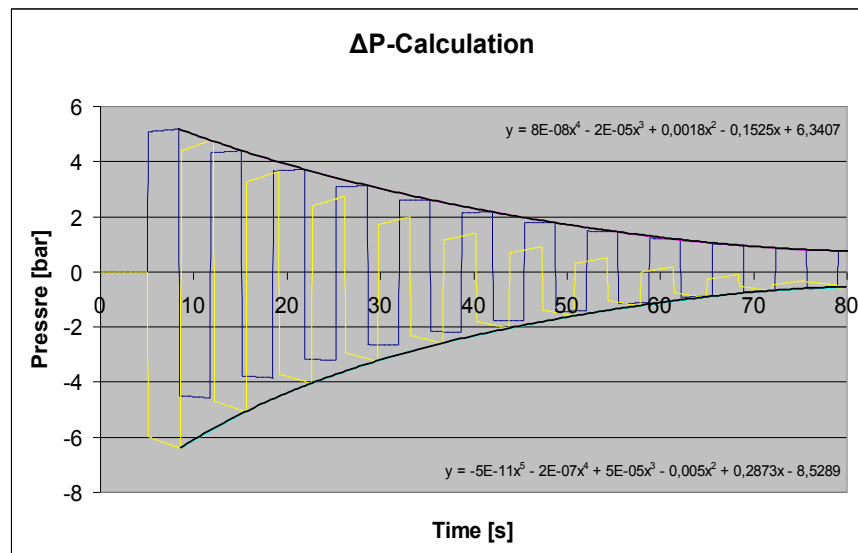


Figure 41: Overlapping of the transient data

The total Δp over time across the casing at the depth of the float collar is illustrated in Figure 42. The sum of the positive and negative Δp -values caused by the water hammer decreases with time till the hydrostatic difference of 50,33bar is left.

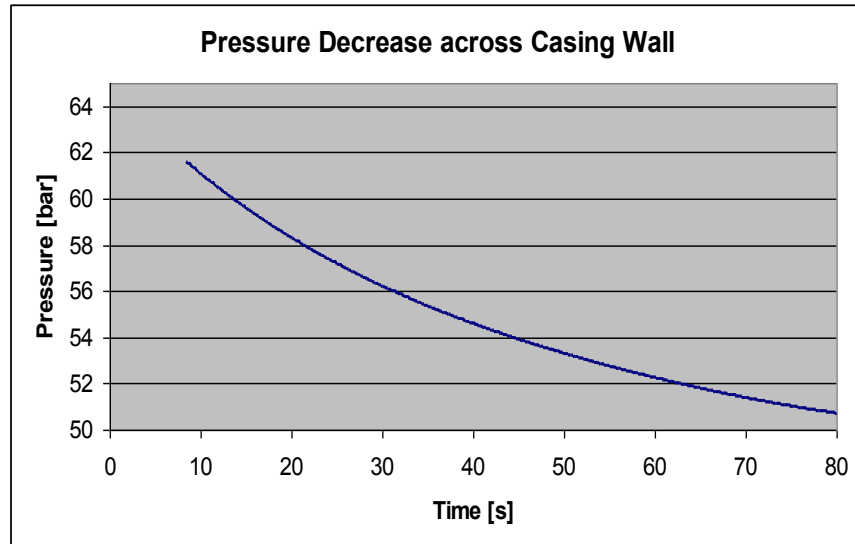


Figure 42: Decreasing Δp acting on the casing

It has to be mentioned that the pressure curve in Figure 42 is an approximation which partly deviates at about 1bar. This deviation can be explained if we take a closer look to Figure 41. For example the values after 20th second do not meet the maximum and minimum curve (Figure 43). At this point of time the sum of the positive and negative Δp value is smaller.

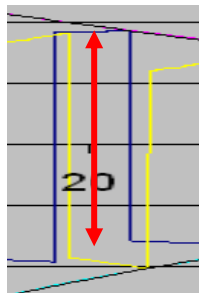


Figure 43: Zoom in of figure 40

In Figure 44 the simulated fluid rate at the casing bond is plotted. For a closer investigation Figure 10 has to be remembered where the pressure wave sequence in a pipe is schematically illustrated and have a closer look to the changing flow direction of the liquid. When the pressure wave is generated and propagates through the pipe the fluid still enters the pipe. This means that after the valve is closed the cement enters the casing as long as the wave takes to arrive at the bond. This time period is calculated by L/c , where L is the pipe length and c is the speed of sound. Therefore the constant discharge rate at the bond lasts nearly 2 seconds longer after the valve is closed. Comparing again with Figure 10 the fluid begins flowing out of the well into the bond when the positive pressure wave starts to travel back down hole. In Figure 44 the reversal in flow direction is shown as the positive discharge rate at steady state conditions switches into negative. This procedure continues and loses its intensity with time. The initial value of $123,6\text{m}^3/\text{h}$ corresponds to the fluid velocity of $0,3\text{m/s}$ in the 16" casing that has a cross-sectional area of $0,114\text{m}^2$. This was calculated on the base of the 12bbl/min free falling rate.

In reality at the cementation of the 16" casing this phenomenon was probably not detected since the free falling zone of 345m was in between the float collar and the cementing head. However, on surface at the annular return lines some irregularities in flow must have taken place if this water hammer occurred down hole.

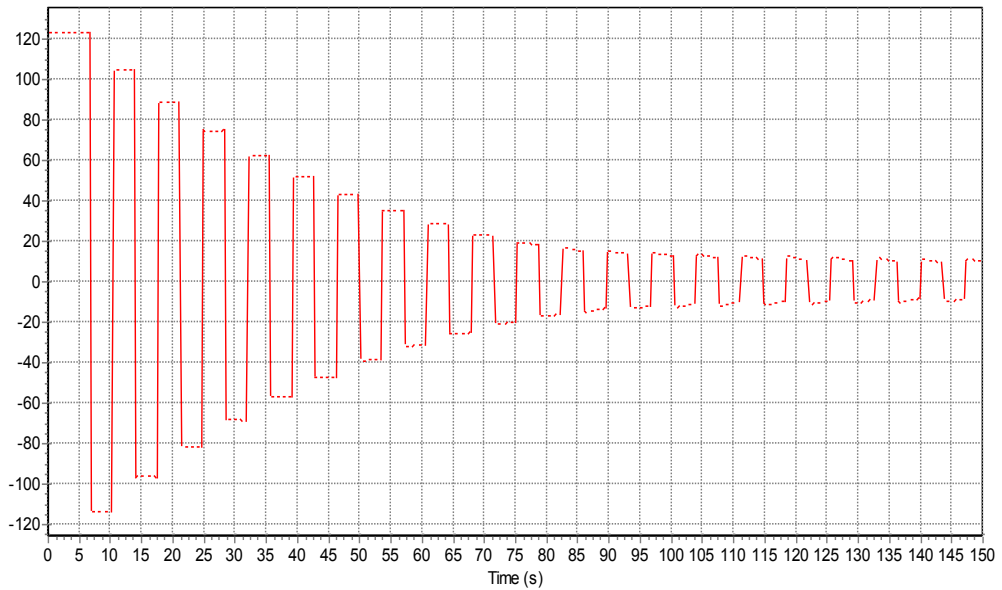


Figure 44: Discharge rate at the casing bond

In Figure the 45 the discharge rate of the annulus is demonstrated. It is a reversal procedure as in Figure 44. As soon as the fluid flow is interrupted the negative pressure wave moves towards the outlet on the surface. During this time (L/c) the discharge at the surface stays constant but when the wave arrives at the outlet and the whole amount of fluid stands still for a tiny moment, the direction of flow is reversed and the fluid enters the “annular” pipe. The fluid flows back into the annulus as long as the pressure wave takes for one time up and down the well. This time period is determined by $2L/c$ (Chapter 7.3.2). This process continues and decreases as the amplitude of the pressure wave decreases. In Figure 45 the initial negative value of $123,6\text{m}^3/\text{h}$ in the steady state period expresses that the fluid enters the bond at surface, a positive value stand for the reversal. After 80 seconds a irregularity can be detected where the wave starts to develop an amplitude again.

In reality a hose was installed at the wellhead that directed the annular returns to the spider box which is installed between the mud return line and the shale shakers to divert the flow. At the outlet of the hose the mud faced atmospheric conditions. When now the negative pressure wave passes the well head and reaches the end of the hose it is reflected at the interface of fluid and air. When the pressure wave turns the mud inside the hose will be forced to flow back towards the well head and since no mud from the spider box can enter air is sucked into the hose. The return rate is interrupted for a duration of 3,6 seconds. The indication at surface would be a repeating break of the return flow and the hose would start to move and vibrate due to the flow and suction sequences. Remarkable occurrences like those were not detected on site.

On the other side in this case it is difficult to estimate the impact on surface equipment and probably since nothing was expected nothing was noticed.

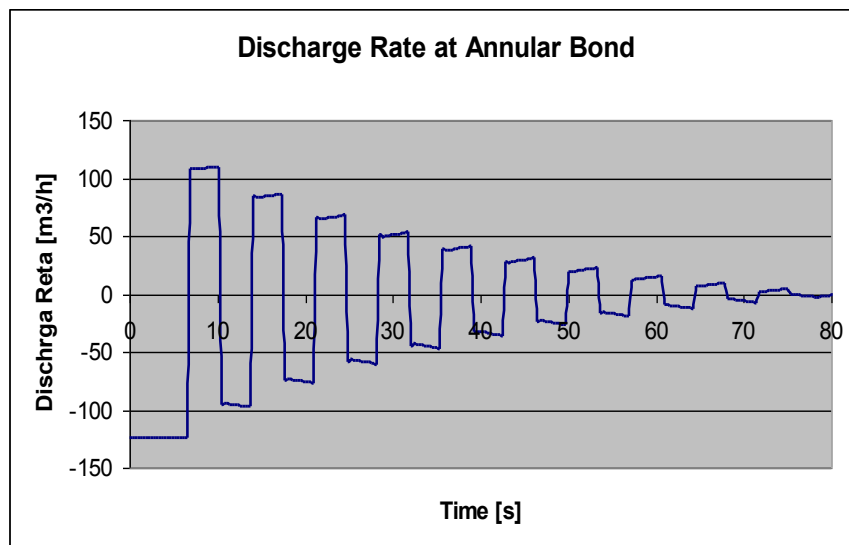


Figure 45: Discharge rate at annular bond

9.4 Analysis – Impact of Different Parameters

Up to now the water hammer theory at OMV's well was investigated and a final result could be found. The maximum load on the casing string was 61.5bar, out of which 11,2bar were caused by the water hammer-effect itself.

The next step is to study how single parameters influence the magnitude of a water hammer. A rather important question is for example in how far the size of the pipe impacts a water hammer? Further more the shape of the pressure curves is investigated. Following parameters that determine a water hammer are discussed in this chapter:

- Friction Force
- Fluid Density
- Fluid Velocity
- Speed of Sound
- Bulk Modulus
- Pipe Dimension

9.4.1 Friction Force

The friction force which is developed due to fluid flow on the pipe wall acts against the direction of flow. If the fluid velocity is zero no friction force occurs. In case of a water hammer the pressure and velocity sequence within the pipe was investigated in a former chapter and is illustrated in Figure 10. If a pressure wave is generated in a pipe and starts to propagate the fluid velocity between the point of generation and the wave front is zero. Therefore the section where no friction force is acting gets longer and longer since the wave front travels towards the pipe inlet. This means the magnitude of the initial generated pressure peak is increased linear with time by the amount of the friction force as shown in Figure 46. When the pressure front reaches the inlet, no friction is acting since the whole fluid column stands still for a moment. The next step is that the wave is reflected and fluid starts to flow out of the pipe. Because of the reverse in flow direction a friction force acting towards the valve is generated. So the pressure at the valve is further increased linear. This effect is responsible for the linear pressure increase at the pressure peak itself. The friction at the pipe wall and the inner friction cause a reduction of the fluid velocity. Due to this reduction the slope of this linear section is getting smaller with the number of pressure wave cycles.

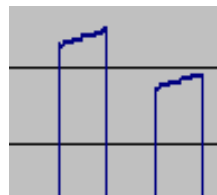


Figure 46: Linear pressure increase due to friction force

Concerning the linear section at the pressure peak it was first assumed that this has to do with the compressibility of the fluid. That's why several runs with different bulk moduli were performed in order to find out if there is a relation between the fluid compressibility and the slope at the pressure peak. The bulk modulus of water ($2,1e9N/m^2$) was doubled and halved for the same boundary conditions. The linear section of each result was then plotted in Excel and the different slopes were determined with regression lines. Figure 47 illustrates the result. In a medium with a lower bulk modulus the speed of sound is much slower and therefore the green line in Figure 47 is the longest. A higher speed of sound results in a higher water hammer effect. That's why the black line is on top.

Regarding the slopes no relation to the different bulk moduli could be detected.

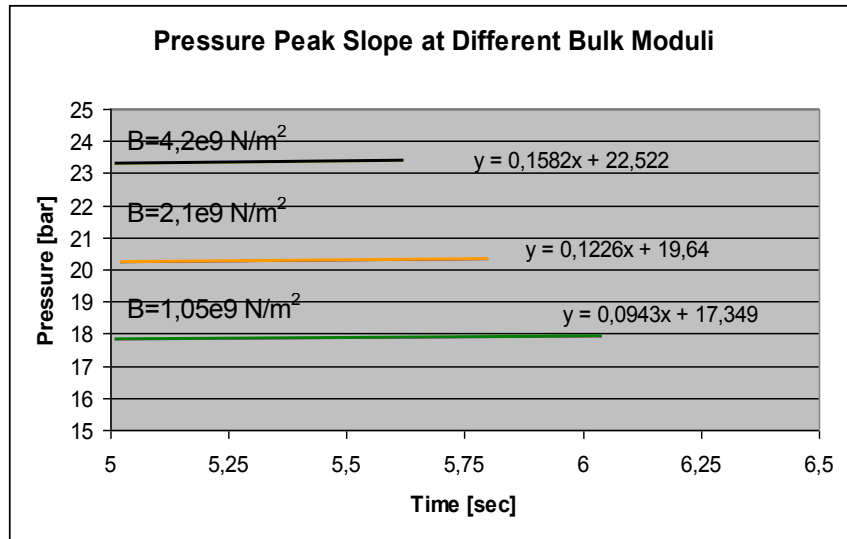


Figure 47: Different bulk moduli affect the slope at the pressure peaks

The relation between the friction pressure and the shape of the pressure peak was noticed when a water hammer in a 7" casing was simulated. In pipes of smaller diameter the friction pressure losses are higher than in those of larger. At the 7" casing the shape of the pressure peak was more significant and the pressure difference of the linear section corresponded to the friction pressure losses.

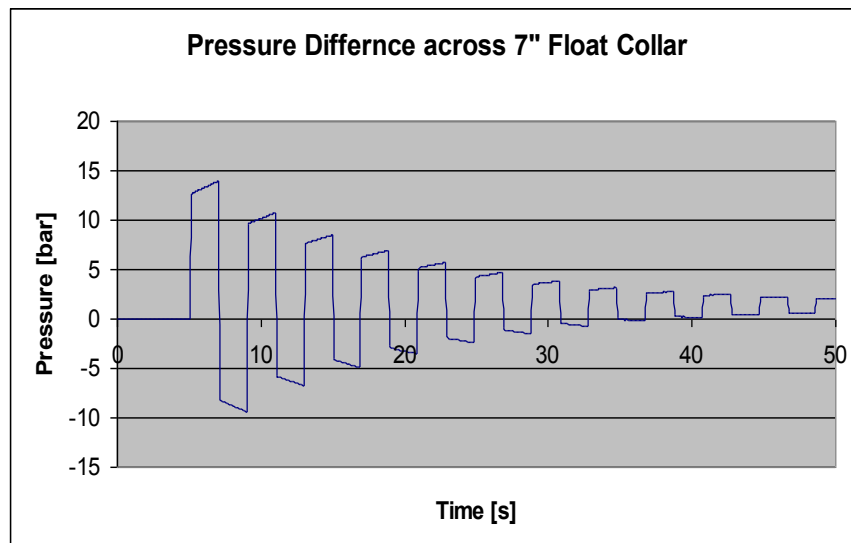


Figure 48: Linear pressure increase on top of pressure peak

The analysis of the next parameters is based on two equations, which were already introduced, the Joukowsky Formula (21) and the speed of sound Formula (22):

$$\Delta p = \rho a \Delta u \quad (21)$$

$$a = \frac{\sqrt{\frac{1}{\rho_F}}}{\sqrt{\frac{1}{E_F} + \frac{D}{t + E_P}}} \quad (22)$$

9.4.2 Fluid Velocity, Fluid Density

The Joukowsky formula shows that by doubling the fluid velocity the Δp before the valve is doubled too. This formula only describes the magnitude of the positive pressure wave, not the total load across a valve. According to Equation (21) the fluid velocity is an important factor. If Δu is doubled, Δp is doubled also. For the simulation of the plug cementation a fluid velocity of 0,3m/s was assumed since 12bbl/min can be assumed as free falling velocity. In Figure 49 the first two pressure peaks of the 16" casing simulation run with a fluid velocity of 0,5 and 1m/s are presented. The remaining boundary conditions were exactly the same. It can be seen that the load across the casing and the valve is significantly increased. The hydrostatic pressure difference of 50,3bar is not considered in Figure 49.

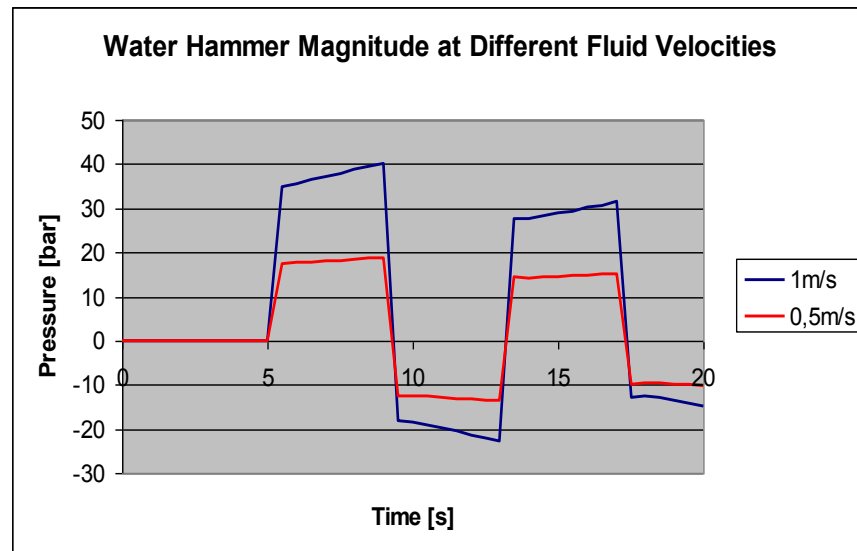


Figure 49: Water hammer simulated with higher fluid velocity

An increase in fluid density causes also a rise of the Joukowsky- Δp although it reduces the speed of sound. This behaviour can easily be understood by applying Equations (21) and (22).

9.4.3 Speed of Sound

The speed of sound is dependent on several different parameters, on the one side the fluid properties density and bulk modulus and on the other side the material properties of the pipe, Youngs modulus, pipe diameter and wall thickness.

In the previous paragraph it was mentioned that increasing fluid density reduces the wave speed. However, the density has a higher power in the Joukowsky equation.

Bulk Modulus

Generally water based fluids are considered as incompressible and this is indeed valid since the volume change due to a certain external pressure is rather small. In case of pressure waves, strictly spoken no material is absolute incompressible. Regarding the wave character of pressure changes a complete incompressible medium would be immediately destroyed because the molecules would not be able to absorb any impact. In case of a liquid flow which causes a water hammer the speed of sound within the liquid is decisive for the magnitude of the pressure peak. In case of a vertical flow a reduction of the liquid column length occurs when the fluid flow is suddenly stopped. In hydraulic engineering the impact of this volume reduction is rather small and therefore not considered. Concerning this topic the author consulted engineers from the Technical University Graz (Austria)¹⁵ who are responsible for the design of hydroelectric power

stations where heads of more than 1000m are not unusual. The presumption that in hydraulic engineering processes water is treated as an incompressible medium was confirmed by the institute of hydraulic engineering at the technical university in Graz¹⁵. In addition to that it was recommended that the bulk modulus of a cement slurry is probably slightly higher as the one of water.

A cement slurry contains solid particles in suspension and in how far this particles influence a water hammer effect can only be figured out by laboratory experiments.

A water hammer determination according to Equations (21) and (22) does not consider the fluid compressibility. However the bulk modulus of a liquid phase plays a decisive role for the determination. It defines the speed of sound in the medium and not the change in liquid volume. Also for the simulation with "Wanda" the compression of a fluid is not taken into account.

In case of the water hammer investigation at the 16" casing the liquid volume change due to pressure can easily be determined by

$$B = \frac{\Delta p}{\frac{\Delta V}{V}} \quad (24)$$

where Δp is the pressure increase and ΔV the volume change of the initial volume V . The total amount of fluid in the wellbore is $236,54\text{m}^3$, the Δp is 5,1bar and the bulk modulus is estimated with $2,4\text{e}9\text{N/m}^2$. The result according to Equation (24) is a volume change of $0,05\text{m}^3$, which is equal to a fluid column of 0,5m. The same result is obtained by using the bulk modulus of water ($2,1\text{e}9\text{N/m}^2$). This result justifies the neglecting of the fluid compressibility.

$$\Delta V = \frac{\Delta p \cdot V}{B} = \frac{5,1\text{e}5 \cdot 236,54}{2,4\text{e}9} = 0,05\text{m}^3$$

Pipe Dimension

The dimension of a pipe is defined by its inner diameter, its length and its wall thickness of the pipe. Equation (22) for the determination of the speed of sound shows in how far these parameters influence the speed of sound and thus the magnitude of the water hammer. The denominator of the equation includes a ratio between the inner diameter and the wall thickness. Comparing several sizes of pipes containing the same liquid the speed of sound must be equal for all, if the D/t ratio is the same. However, if the wall thickness stays constant and only the inner diameter is increased the wave velocity would be reduced as the value of the denominator rises. A reduction of the speed of sound within a fluid reduces the Δp after Joukowsky. Therefore following Equation (22) it can be said that in pipes with a bigger wall thickness the magnitude of a water hammer is smaller. A larger diameter does not lead to a stronger water hammer but reduces the pressure wave speed and therefore reduces the water hammer effect. This statement is valid if all boundary conditions stay the same, also the volumetric ratio between mud and cement. Regarding the analysis of the impact of the pipe dimension on the magnitude of the water hammer several pipe sizes were simulated. For each pipe length three different diameters were tested, whereas all pipes had the same wall thickness. The pipes were simulated horizontally and water at a velocity of 0,5m/s is flowing through until a valve is closed within 0,02 seconds. The pipe length listed in Table 3 is the length before and after the valve. Recorded is the total pressure difference across the valve.

Pipe Length [m]	Inner Diameter [mm]	Wall Thickness [mm]	Δp [bar] after Joukowsky
400	200	12	6,71
	400	12	6,27
	600	12	5,92
600	200	12	6,71
	400	12	6,27
	600	12	5,92
800	200	12	6,71
	400	12	6,27
	600	12	5,92

Table 3: Simulated pipe dimensions

The results are shown in the following pages. Indeed the discussed trend in loading which was based on the Equations (21) and (22) can also be noticed at the different runs. At a constant wall thickness an increasing diameter causes a lower Δp across the valve. This is valid for each length. In order to show that the trend of the simulation is true the fourth column in Table 3 presents the results calculated by Joukowsky. In the equation the length does not play a role. In the following figures the height of the first pressure peak of those pipes with the same length should be compared.

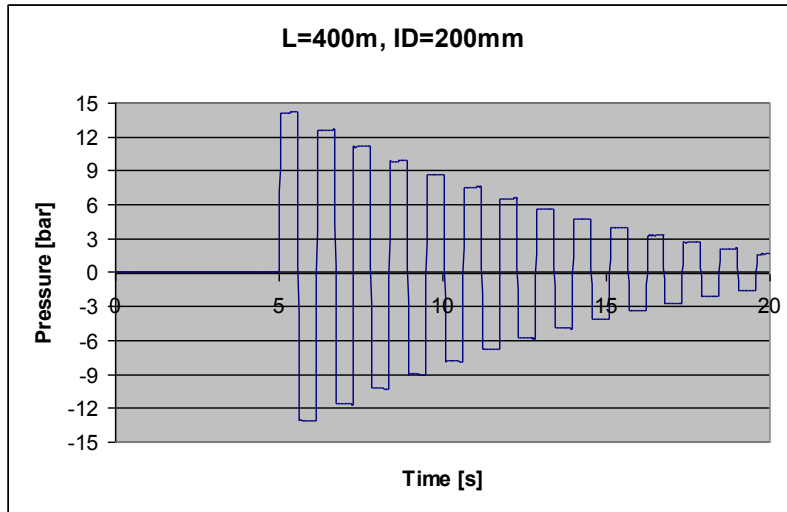


Figure 50: Pipe dimension test 1/9 (L=400m, ID=200mm)

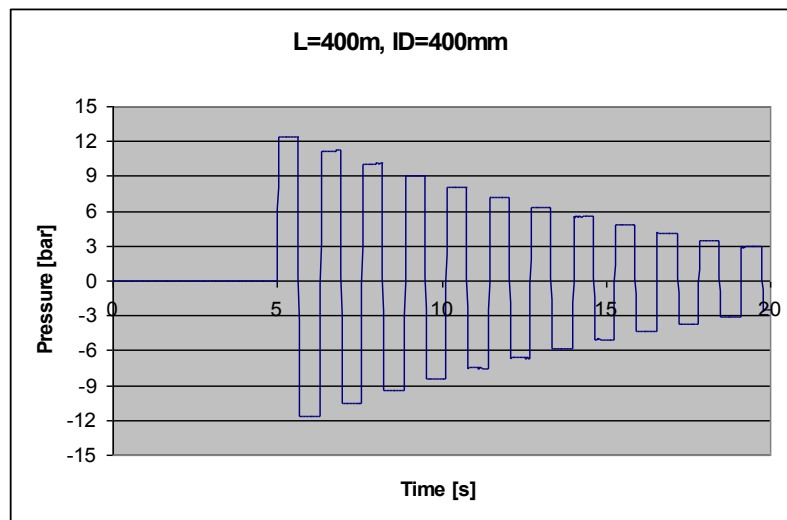


Figure 51: Pipe dimension test 2/9 (L=400m, ID=400mm)

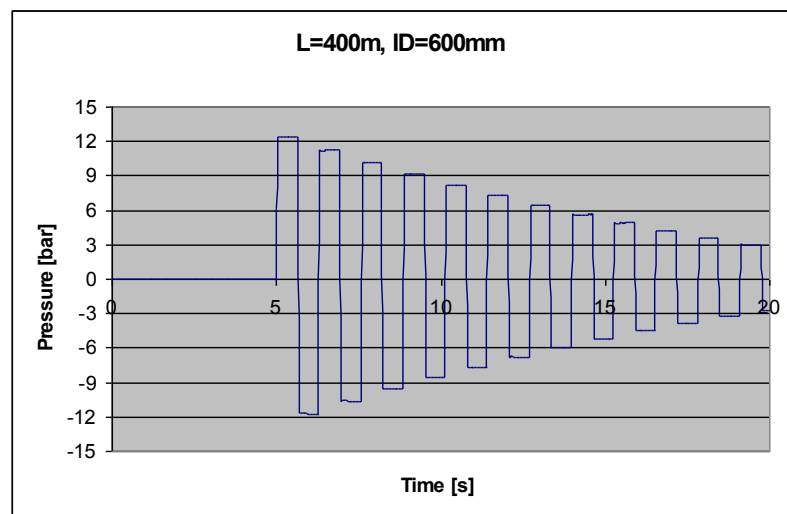


Figure 52: Pipe dimension test 3/9 (L=400m, ID=600m)

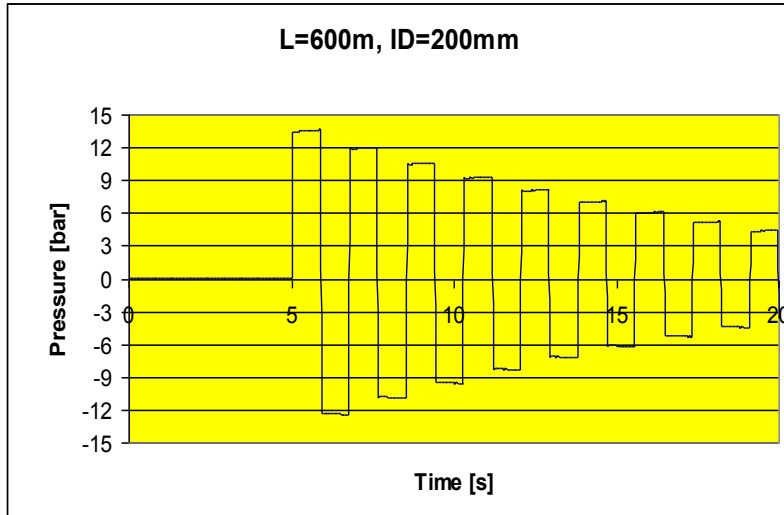


Figure 53: Pipe dimension test 4/9 (L=600m, ID=200mm)

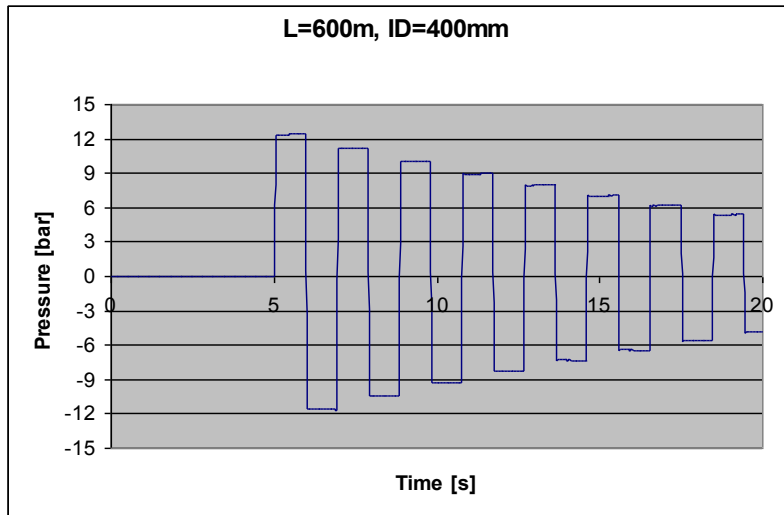


Figure 54: Pipe dimension test 5/9 (L=600, ID=400mm)

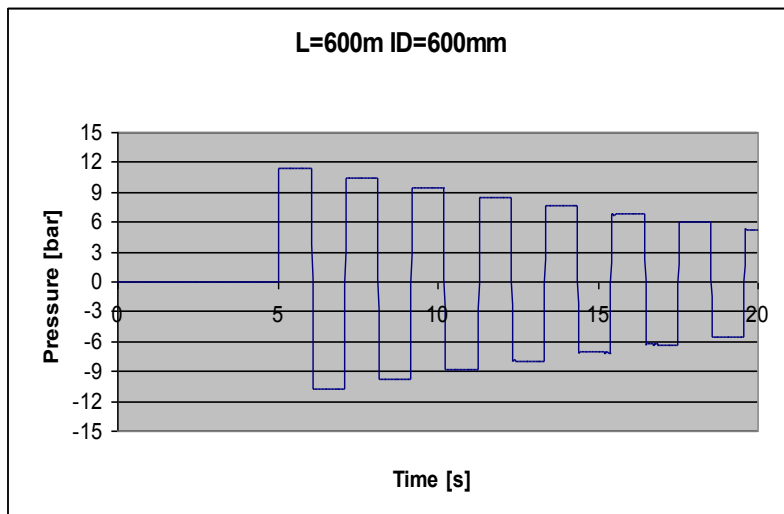


Figure 55: Pipe dimension test 6/9 (L=600m, ID=600mm)

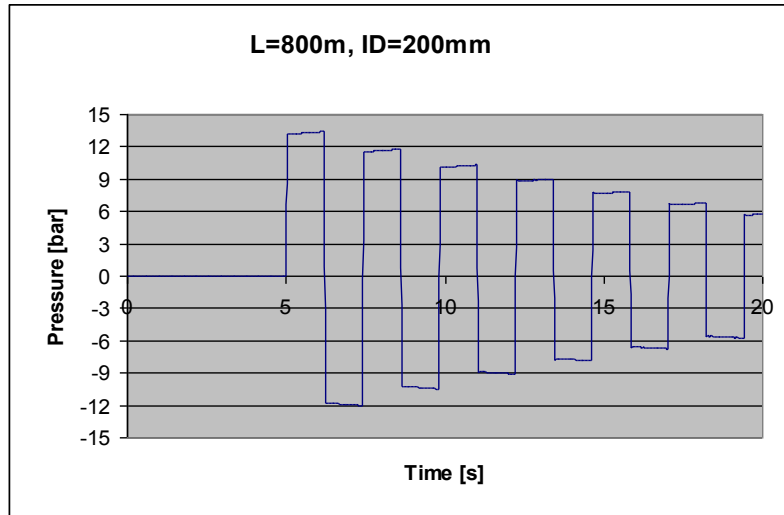


Figure 56: Pipe dimension test 7/9 (L=800m, ID=200mm)

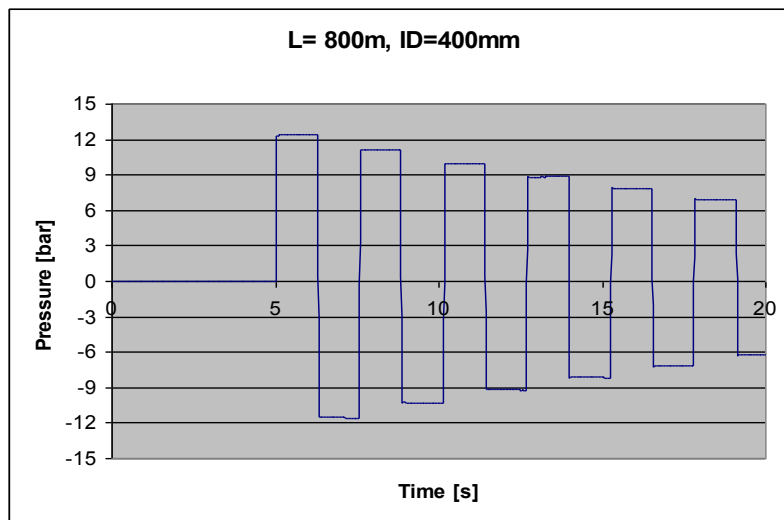


Figure 57: Pipe dimension test 8/9 (L=800m, ID=600mm)

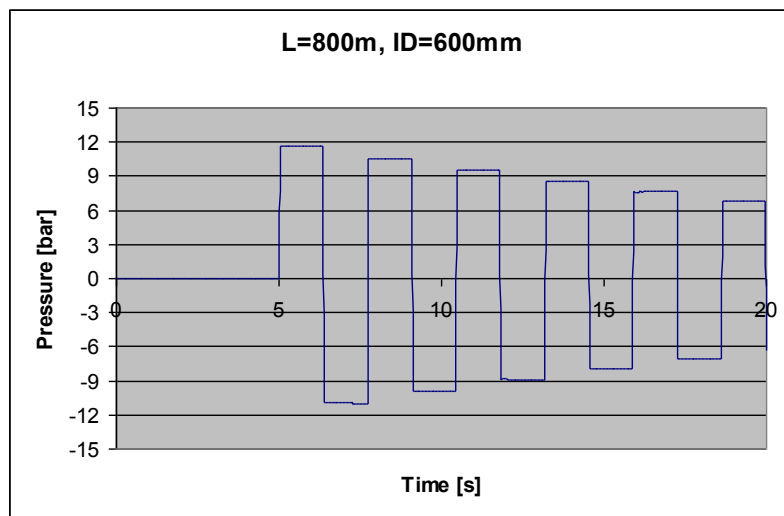


Figure 58: Pipe dimension test 9/9 (L=800m, ID=600mm)

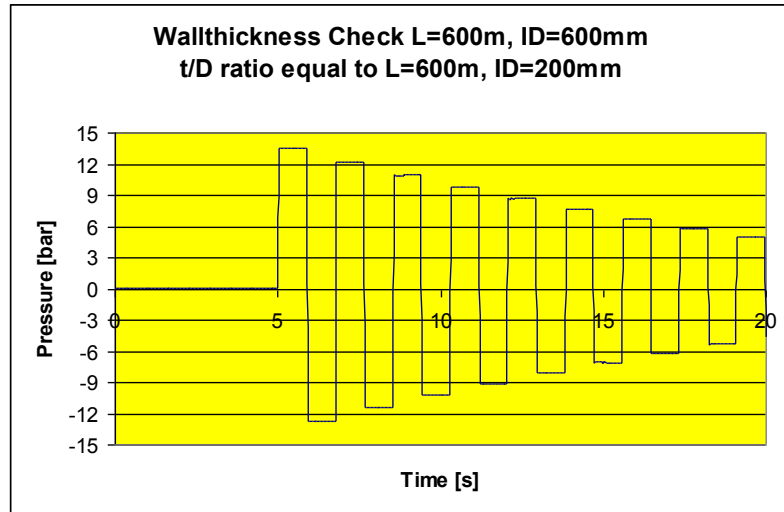


Figure 59: Pipe dimension test regarding wall thickness

Figures 53 and 59 with the yellow background further prove the assumption regarding the pipe wall thickness. The pipe in Figure 53 has a wall thickness of 12mm, equal to the others, so its ID/t ratio r is:

$$r = \frac{200}{12} = 16,6$$

Now the pipe from Figure 59 (ID=600mm) was simulated with the same ID/t ratio like the one from Figure 53:

$$r = \frac{600}{35,9} = 16,6$$

The magnitude of the water hammer is in both cases 16,5bar.

About the impact of the pipe length no statement was made up to now. For the determination after Joukowsky the pipe length does not play any role for the magnitude of the Δp . Following this a change length does not influence the water hammer. The longer the pipe the longer it takes the pressure wave to travel back and forth. This can be seen in Figures 50 to 58 since the single pressure peaks are getting broader. Even from the simulation no clear trend in how far the pipe length is related to the height of the pressure peaks can be detected. All pipes with the internal diameter of 400mm show the same result, illustrated in Figures 51,54 and 57. The remaining ones tend to decrease slightly. An increase of the water hammer effect with an increase of pipe length at same boundary conditions can not be detected.

After these investigations the author was interested into an unrealistic but interesting example. What would be the result if the 16" casing string was 10.000m long?

The previous simulation set up was changed to a depth of 10.000m and the run was simulated with the cement slurry only. The result is shown in Figure 60. It can be seen that the load due to the water hammer is far away from endangering the casing to burst. The effect of friction can be seen very clearly from the linear section of the pressure peaks.

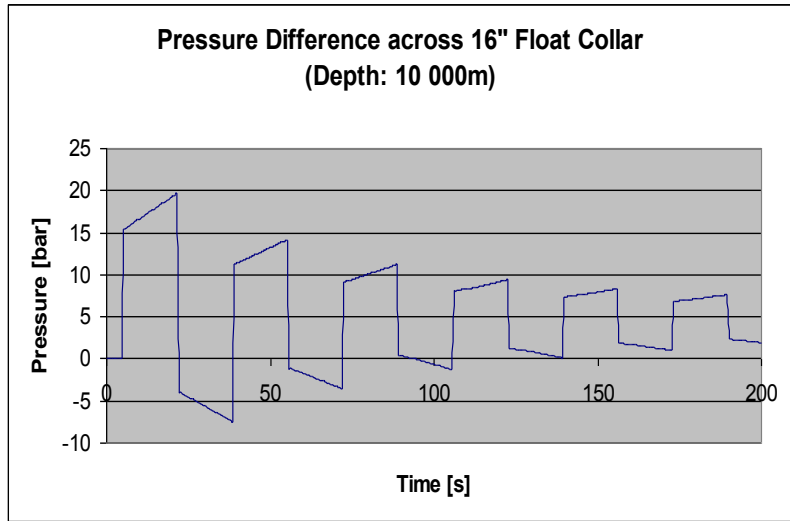


Figure 60: Water hammer effect if the well would have been 10.000m deep

10. Limits of Different Casing Sizes

At OMV a water hammer probably occurred during the plug cementation of the 16" casing string. The task of this chapter is to find out the limits of common casing sizes, for the case that a plug cementation again generates a water hammer due to any defects.

On base of the previous investigations the relation between pipe size and water hammer magnitude is known. Further more all parameters that influence the height of the pressure peak are well known:

- Fluid density
- Fluid velocity
- Speed of sound
- Bulk modulus
- Youngs modulus
- Pipe diameter
- Wall thickness

The question is which parameters are planned ahead and which can be influenced directly. In the casing design process the type and size of the string is chosen long before the well is drilled. Since the casing is selected the pipe properties Youngs modulus, diameter and wall thickness can be considered as constants. The bulk modulus of the slurry can also be seen as a constant because it cannot be significantly changed except for foamed slurries. Density has a rather high impact on the water hammer phenomenon. Concerning the slurry density the author decided to select the same density as it was used for the investigation of the 16" casing cementation. The composition of the slurry used was a quite common one and further the value determined for the simulation includes the volumetric ratio of mud, lead and tail cement. The slurry velocity is equal the free falling velocity which can only be reduced if a back up pressure is provided at the annular return.

In the following for common casing diameters the maximum allowable flow rate is figured out. Above this critical value a water hammer would exceed the burst resistance of the different casings.

Following casing sizes were tested:

OD [in]	Weight [lb/ft]	Grade	Wall thickness [in]	Internal Yield Pressure [psi]
7"	29	TN 95HS	0,40	9690
9 5/8"	53,5	API L80	0,54	7930
13 3/8"	80,7	TN 95HS	0,58	7210
16"	84	API L80	0,49	4330
20"	106	API J55	0,50	2420

Table 4: Tested casing sizes

Size [in]	7"	9 5/8"	13 3/8"	16"	20"
Depth [m]	Slurry velocity [m ³ /min]				
1000	4,65	15,5	43,5	41,01	43,9
2000	3,6	12,18	33,71	32,18	36,2
3000	3,14	10,65	29,36	28,07	32,92
4000	2,9	9,52	27,18	26,02	29,63

Table 5: Critical slurry velocities for different casing sizes

From Table 5 a decrease of the critical pump rate with increasing depth can be noticed for

all casing size. This can be explained due to friction forces. The deeper the casing the higher is the friction pressure loss. For a water hammer calculation this loss again appears as the linear pressure increase on top of the pressure peak itself. Concerning the internal yield pressure this additional Δp is high enough to “allow” the fluid velocity to be reduced. For the same depth the tendency of different pipe sizes is illustrated in Figure 61. As mentioned before it can be seen that the deeper the well the lower would be the critical flow rate. This is valid for all casing sizes. Concerning the diameter the critical flow rates above 13 3/8” casings do not differ that much compared to 7” and 9 5/8” casings. The simulation runs for these casing size tests were performed as U-tubes. The inner diameter of the annular pipe was determined by the ratio of the hole diameter to the outer diameter of the 16” casing.

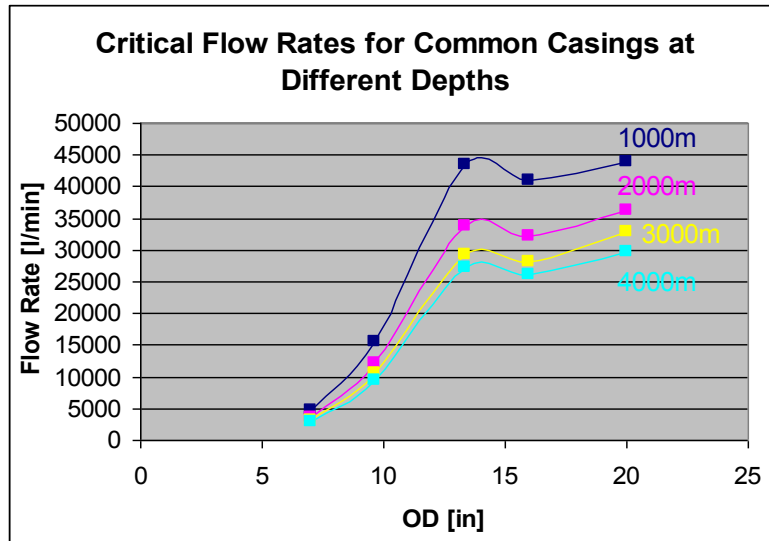


Figure 61: Tendency of the critical flow rate for several casings at certain depths

11. Conclusion

First of all, why was the water hammer theory taken into consideration?

A water hammer only occurs if a fluid flow is stopped immediately. Concerning the plug cementation it is a realistic assumption that the bottom plug which was made out of rubber faced so much wear on its way downhole that it was decomposed. Therefore a plugging of the valve could be possible. It is even known that bottom plugs might turn around while they are pumped downhole. Of course this is also a question of plug quality.

The simulation of the water hammer-effect at the 16" casing delivered a maximum pressure difference of 61,53bar across the casing wall whereas 50,33bar out of this is caused by the hydrostatic difference between the casing and the annular. Only 11,6bar are generated by the impact of the water hammer and as it can be seen from Figure 62 this is the amount of pressure that is reduced with time. It is remarkable that this impact is rather small. It is obvious that the total load does not endanger the 16" casing string to burst.

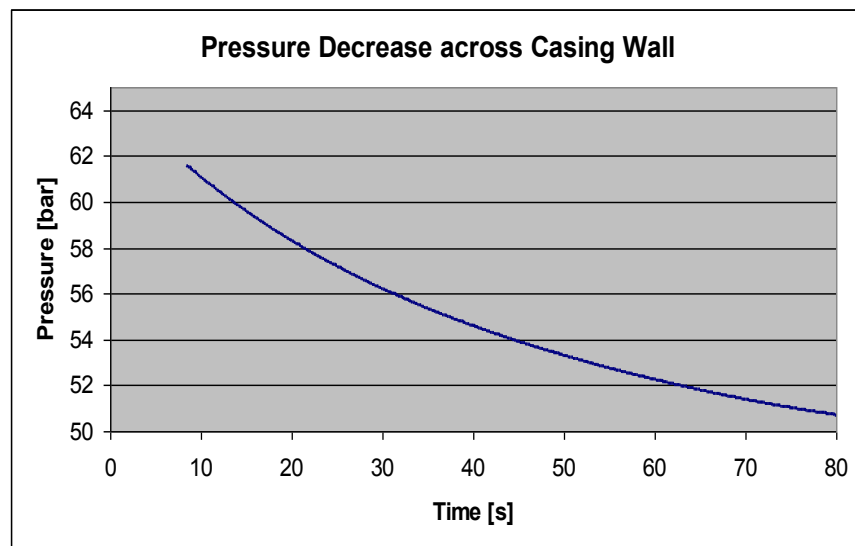


Figure 62: Δp caused by water hammer acting on the casing

This result seems to be an approach for further investigation of the problem occurred in OMV well during the 16" cement job. A special topic like the connection slippage theory would be worth to be studied in detail since it was not included in this thesis. Concerning this further theory the impact of the slurry velocity which was shown in Figure 49 has to be pointed out.

Concerning the casing dimension its impact on the water hammer magnitude could be proved mathematically and by the simulation. For a constant wall thickness a larger inner diameter reduces the speed of sound and thus the generated Δp . The reverse happens in case of a smaller diameter. In pipes of different sizes but with same D/t ratio the magnitude of a water hammer is equal for each diameter. It was shown that pipes with a larger wall thickness face a higher load if water hammer occurs.

Pipe length or depth only indirectly influences the resulting Δp . The amount of friction pressure losses in a longer pipe section is higher as in a shorter one of course. Friction pressure losses lead to a further but linear increase of the pressure peak with time. This means the maximum pressure is reached after the time $2L/a$, with L as pipe length and a as speed of sound. This behaviour is related to the pressure and velocity sequence in the pipe when the pressure wave is reflected.

Figure 61 represents the flow rate limit above which common types of casings are endangered to burst when a water hammer occurs at a certain depth. Very general spoken in deeper wells the burst resistance of a casing is exceeded at lower fluid velocities as in case of shallower wells.

The initial assumption that the compressibility of the slurry column has a significant impact on the final water hammer load could not be confirmed by this investigation. It was determined that the slurry column length was reduced by half a meter due to liquid compression. Following the calculation this rather small impact can be neglected. In this context it has to be pointed out that a slurry contains solid particles. It is not clear whether these particles influence the compressibility

Regarding the simulation it must be said that computational programs strictly follow physical laws and formulas. Therefore results are based on ideal conditions. The fact that the slurry contains solid particles can not totally be covered by the simulation. Slurries viscosity is a known parameter whereof the kinematic viscosity can be determined. The viscosity of a liquid is based on the interaction of molecules. This interaction causes inner friction since it counteracts on movement and thus is responsible for the shear stress - shear rate relation of a liquid. Due to the known viscosity the inner friction of the slurry and its solid particles are considered in the simulation.

Concerning the pressure wave velocity it is known that small gas bubbles dispersed in a fluid reduced the speed of sound significantly. It is assumed that the opposite would be true for solid particles if they were homogeneously arranged and in direct contact to each other¹⁵. Since this is not the case in a suspension the solid particles do not increase the speed of sound. In how far they in fact influence the wave propagation velocity was not investigated during this thesis.

For the height of the first pressure peak the inner friction is irrelevant but not for the decline of the following pressure peaks. The inner friction strongly dampens the pressure wave intensity. The simulation delivered a pressure sequence that lasted about 80 seconds. In hydraulic engineering at the Technical University Graz (Austria) the experience was made that the duration of a pressure sequence after a water hammer is in reality shorter as it is determined by a simulation. However, it can only be assumed how long it actually lasted.

10. References

- 1 Spörker, H.: "Analysis of the Free Fall Phenomenon During Primary Cementing", Thesis, Leoben U., Austria (1993)
- 2 Beirute, R.M.: "The Phenomenon of Free Fall During Primary Cementing", SPE 13045, 1984; "A Technique for Onsite Diagnosis of Cement Job Problems: The Concept of Job Signature", SPE 16649, 1987
- 3 Science and Technology Encyclopedia: "Water Hammer", <http://www.answers.com/topic/water-hammer>, 01.02.2007
- 4 Klasinc, R.: "Hydraulic VA", Script, Technical University Graz, Austria,
- 5 Pickford, J.: "Analysis of Water Surge" 1969, Gordon and Breach Science Publisher, http://www.nesc.wvu.edu/ndwc/articles/ot/WI03/Water_Hammer.html, 01.02.2007
- 6 Repp, T.: "Fluiddynamic Waterhammer Simulations with Consideration of Fluid-Structure Interaction", Publication presented at the annular conference of nuclear science in Karlsruhe, Germany, Mai 1999, <http://www.fzd.de/publications/002143/jb08.pdf>, 01.02.2007
- 7 Tipler, P.: "Physik", (2000), p. 459-470
- 8 Wikipedia Encyclopedia: "Schallgeschwindigkeit" <http://de.wikipedia.org/wiki/Schallgeschwindigkeit>, 01.02.2007
- 9 Tipler, P.: "Physik" (2000), p. 207
- 10 Wikipedia Encyclopedia: "Innere Reibung", http://de.wikipedia.org/wiki/Reibung#Innere_Reibung, 01.02.2007
- 11 HyperPhysiks, Georgia State University: <http://hyperphysics.phy-astr.gsu.edu/hbase/permot3.html>, 01.02.2007
- 12 Wikipedia Encyclopedia: "Bulk Modulus", http://en.wikipedia.org/wiki/Bulk_modulus, 01.02.2007
- 13 Wikipedia Encyclopedia: "Cavitation", <http://en.wikipedia.org/wiki/Cavitation>, 01.02.2007
- 14 Tenaris Oilfield Services, Online Catalogue: <http://www.tenaris.com/archivos/documents/2003/532.pdf>, 01.02.2007
- 15 Univ.-Prof. DI. Dr. techn. Heigerth Günther, DI Dr. techn. Dominik Mayr